Identification of Piperazinylbenzenesulfonamides as New Inhibitors of Claudin-1 Trafficking and Hepatitis C Virus Entry

Laura Riva, Ok-Ryul Song, Jannick Prentoe, Francois Helle, Laurent L'Homme, Charles-Henry Gattolliat, Alexandre Vandeputte, Lucie Fénéant, Sandrine Belouzard, Thomas F. Baumert, et al.

IDENTIFICATION OF PIPERAZINYLBENZENESULFONAMIDES AS NEW INHIBITORS OF CLAUDIN-1 TRAFFICKING AND HEPATITIS C VIRUS ENTRY

Laura Riva[1*§], Ok-ryul Song[1], Jannick Prentoe[2], François Helle[3], Laurent L'homme[4], Charles-Henry Gattolliat[5,6,7], Alexandre Vandeputte[1], Lucie Fénéant[1#], Sandrine Belouzard[1], Thomas F. Baumert[8], Tarik Asselah[5,6,7], Jens Bukh[2], Priscille Brodin[1], Laurence Cocquerel[1], Yves Rouillé[1], Jean Dubuisson[1*]

Univ. Lille, CNRS, Inserm, CHU Lille, Institut Pasteur de Lille, U1019-UMR 8204-CIIL-Centre d'Infection et d'Immunité de Lille, Lille, France[1]
Copenhagen Hepatitis C Program (CO-HEP), Department of Infectious Diseases and Clinical Research Centre, Hvidovre Hospital and Department of Immunology and Microbiology, Faculty of Health and Medical Sciences, University of Copenhagen, Copenhagen, Denmark[2]
EA4294, Laboratoire de Virologie, Centre Universitaire de Recherche en Santé, Centre Hospitalier Universitaire et Université de Picardie Jules Verne, Amiens, France[3]
Univ. Lille, Inserm, CHU Lille, Institut Pasteur de Lille, U1011-EGID, F-59000 Lille, France[4]
INSERM, UMR1149, Team «Physiopathologie et traitements des hépatites virales», Centre de Recherche sur l'Inflammation, and Université Denis Diderot Paris 7, site Bichat, BP 416, F-75018, Paris, France[5]
Service d'hépatologie, PMAD Hôpital Beaujon, 100 Bd du Général Leclerc, Clichy la Garenne, 92110 Clichy Cedex, France[6]
Laboratory of Excellence Labex INFLAMEX, PRES Paris Sorbonne Cité, Paris, France[7]
Inserm, U1110, Institut de Recherche sur les Maladies Virales et Hépatiques, Université de Strasbourg, Strasbourg, France[8]

Running Head: 5-HT6 inhibitors affect CLDN1 export and HCV entry

* Address correspondence to jean.dubuisson@ibl.cnrs.fr, laura.riva@alumni.ulg.ac.be

§ Present address: Immunity and Pathogenesis Program, Infectious and Inflammatory Disease Center, Sanford Burnham Prebys Medical Discovery Institute, 10901 North Torrey Pines Road, La Jolla, California 92037, USA.
# Present address: Department of Cell Biology, University of Virginia School of Medicine, Charlottesville, Virginia, USA

Keywords: Hepatitis C virus; virus entry; virus-host interaction; protein kinase A; tight-junction protein

41 **ABSTRACT**

42 Hepatitis C virus (HCV) infection causes 500,000 deaths annually, associated with end-stage
43 liver diseases. Investigations of the HCV life cycle widened the knowledge in virology, and
44 here we discovered that two piperazinylbenzenesulfonamides inhibit HCV entry into liver
45 cells. The entry process of HCV into host cells is a complex process, not fully understood, but
46 characterized by multiple spatially and temporally regulated steps involving several known
47 host factors. Through a high-content virus-infection screening analysis with a library of 1,120
48 biologically active chemical compounds, we identified SB258585, an antagonist of the
49 serotonin receptor 6 (5-HT6), as a new inhibitor of HCV entry in liver-derived cell lines, as
50 well as in primary hepatocytes. A functional characterization suggested a role for this
51 compound, as well as for the compound SB399885 sharing a similar structure, as inhibitors of
52 a late HCV entry step, modulating the localization of the co-receptor tight junction protein
53 claudin 1 (CLDN1), in a 5-HT6 independent manner. Both chemical compounds induced an
54 intracellular accumulation of CLDN1, reflecting export impairment. This regulation
55 correlated with the modulation of protein kinase A (PKA) activity. The PKA inhibitor H89
56 fully reproduced these phenotypes. Furthermore, PKA activation resulted in increased
57 CLDN1 accumulation at the cell surface. Interestingly, increase of CLDN1 recycling did not
58 correlate with an increased interaction with CD81 or HCV entry. These findings reinforce the
59 hypothesis of a common pathway shared by several viruses, which involves G-protein
60 coupled receptor -dependent signaling in late steps of viral entry.

61 **IMPORTANCE**

62 The HCV entry process is highly complex and important details of this structured event are
63 poorly understood. By screening a library of biologically active chemical compounds, we
64 identified two piperazinylbenzenesulfonamides as inhibitors of HCV entry. The mechanism
65 of inhibition was not through previously described activity of these inhibitors as antagonists

of the serotonin receptor 6, but instead through modulation of PKA activity in a 5-HT6 independent manner, as proven by the lack of 5-HT6 in liver. We thus highlighted the involvement of PKA pathway in modulating HCV post-binding step entry and in the recycling of the tight junction protein claudin-1 (CLDN1) towards the cell surface. Our work underscores once more the complexity of HCV entry steps and suggests a role for PKA pathway as regulator of CLDN1 recycling, having an impact on both cell biology and virology.

INTRODUCTION

Virus entry into specific host cells is a tightly regulated multistep process. Among known viruses, the liver pathogen hepatitis C virus (HCV), which causes 500,000 deaths annually, has probably one of the most complex multistep entry processes involving a growing number of cellular entry factors (1). Furthermore, the regulation of trafficking of these proteins provides an additional level of complexity. Although the involvement of a large number of host factors has been demonstrated in HCV entry, several gaps remain in our comprehension of this process. Further functional studies are therefore needed to better understand the regulation of the early steps of the HCV life cycle.

After binding to attachment factors such as heparan sulfate proteoglycans and the low density lipoprotein (LDL) receptor, HCV particles specifically bind to the entry receptors scavenger receptor BI (SRB1) and CD81 tetraspanin (2). HCV binding to CD81 induces a diffusion of this virion-tetraspanin complex on the plasma membrane, towards the sites of viral internalization (3). Only a specific fraction of CD81, located outside of tetraspanin-enriched areas, is involved in HCV entry (4) through its interaction with the tight junction protein claudin 1 (CLDN1) (5–7). Importantly, CD81-CLDN1 interaction is a major event driving HCV endocytosis (8). Among other identified host factors involved in HCV entry (2),

occludin (OCLN), another tight-junction protein, also plays a major role in a late step of HCV entry through an unknown mechanism (9). Together, these observations indicate that tight junction proteins play a central role in HCV entry. However, the regulation of these proteins in the liver remains poorly understood and little information is available on CLDN1 trafficking and its interplay with CD81 and OCLN both in infected and non-infected cells.

In this study, we implemented a high-content screening (HCS) approach using a library of chemical compounds to search for new regulators of HCV entry. We identified serotonin receptor 6 (5-HT6) antagonists SB258585 and SB399885 as inhibitors of a late step of HCV entry. More specifically, we showed a reduction of PKA activation upon treatment, in a 5-HT6-independent manner. We confirmed the involvement of PKA pathway in HCV entry and a role of its activation in CLDN1 export. Taken together, these data identify new inhibitors of HCV post-binding step and provide new findings in regulation of CLDN1 transport and function. This work highlights once more the complexity of the HCV entry process proving that the presence of CLDN1 at the cell surface is not sufficient to mediate its interaction with CD81. This confirms the importance of the membrane environment and the need of the synergistic action of several receptors in HCV entry.

RESULTS

Identification of the 5-HT6 antagonist SB258585 as a new inhibitor of the HCV life cycle.

To identify new cellular factors involved in the early steps of the HCV infectious cycle, we performed a HCS using a library of 1,120 biologically active chemical compounds. The screen was repeated using three different concentrations (1 μM, 10 μM and 20 μM) in Huh-7 cells infected with cell culture derived HCV (HCVcc) strain JFH1 (genotype 2a) (10, 11). A re-infection experiment was performed as an additional filter to eliminate false-

positive compounds (Supplemantal dataset S1). Compounds reducing the infection by at least 45% compared to the average of DMSO wells affecting cell viability for less than 35% were considered as positive hits (Fig. 1A-C). Finally, we only retained compounds confirmed in the re-infection experiment and inhibiting HCV infection for at least two of the three tested concentrations (Fig. 1D and Table 1). According to these criteria, 20 compounds were selected. Nine of them had been previously described as having an inhibitory effect on HCV or targeting cellular pathways identified as important for HCV infection, thus validating our screen (12–16). Among the 11 remaining hits, we identified 5 compounds targeting serotonin (5-HT) receptors or transporters. Serotonin receptors constitute a class of 16 human receptors, none of which have ever been identified as host factor involved in the HCV infectious cycle. To identify the 5-HT receptor(s) playing a role in HCV infection, we searched the Tocriscreen Total library for all the compounds targeting in a more or less specific manner each of these receptors, in accordance with data available on the following databases: http://www.guidetopharmacology.org/ and http://stitch.embl.de (17). Interestingly, with only one exception, all the compounds targeting the serotonin receptor 6 (5-HT6) showed a dose-response inhibitory effect on HCV JFH1 infection (Fig. 1E), in contrast to the compounds targeting other 5-HT receptors where, for most of them, only the highest concentration showed an inhibitory activity. Among the inhibitors of 5-HT6, SB258585 was identified as a hit according to the criteria of lack of cell toxicity and inhibition of infection chosen in the screen (Fig. 1F and Table 1).

SB258585 inhibits HCV infection, down-regulating PKA activity independently of 5-HT6 receptor.

In order to confirm the inhibitory effect of 5-HT6 antagonist SB258585 on HCV viral cycle, kinetics of JFH1 infection were performed in the presence of this compound. The

141 maximum inhibitory effect of SB258585 was observed when the chemical compound was
142 added during the inoculation of the virus (Fig. 2A), suggesting an effect on virus entry. As
143 shown in Fig. 2B, the inhibition was not due to drug toxicity.
144 5-HT6 receptor, mainly studied in the central nervous system, has not been
145 characterized in the liver or hepatocyte. In order to determine its real involvement in HCV
146 infection as a target of SB258585, we quantified its expression level in the liver. To do so, we
147 compared its distribution by qRT-PCR in seventeen different human tissues. This analysis
148 showed that 5-HT6 was highly expressed in brain tissues and intestine (Fig. 2C). It was also
149 expressed in testis, while it was not detected in all the other tissues, including the liver (Fig.
150 2C). Quantification of 5-HT6 mRNA in Huh-7 cells by qRT-PCR showed a ΔCt of around 18
151 as compared to the housekeeping gene RPLP0, confirming an almost complete absence of
152 detection of 5-HT6 in this hepatic cell line. Not surprisingly, we were unable to detect the 5-
153 HT6 protein by western blot and flow cytometry by using different antibodies (data not
154 shown). This observation implies that the effect observed on HCV infection is probably not
155 connected to 5-HT6.
156 5-HT6 is a G-protein coupled receptor (GPCR), associated with a G alpha stimulatory protein
157 (Gαs). This Gαs activates the adenylyl cyclase to produce cAMP, which in turn activates
158 protein kinase A (PKA) (18). However, GPCR agonists and antagonists often show affinity
159 for additional GPCR than the one specifically targeted. Therefore, we evaluated whether the
160 presence of 5-HT6 antagonist leads to a regulation of the PKA pathway, likely through
161 modulation of other GPCRs. We thus performed a western blot with an antibody specific for
162 PKA phosphorylated substrates. The cell permeable inhibitor of cAMP-dependent protein
163 kinase (PKA) H89 was used as a positive control. This compound is described to inhibit PKA
164 by competitive binding to the ATP site on PKA catalytic subunit (19). As shown in Fig. 2D,

SB258585 reduced the phosphorylation level of PKA substrates in a similar manner as the PKA inhibitor H89.

Therefore, our observations about the phosphorylation level of PKA substrates suggest that the off-target effect of SB258585 targets a factor involved in PKA activation, likely another GPCR coupled to a Gαs protein.

SB258585 and SB399885 inhibit a late step of HCV entry, altering cell surface localization of CLDN1.

According to the kinetics shown in Fig. 2A, SB258585 seems to inhibit HCV entry. The inhibitory effect of SB258585 on HCV entry was then validated with the help of retroviral pseudo-particles harboring HCV envelope glycoproteins (HCVpp) from JFH1strain (genotype 2a) (Fig. 3A). SB258585 had no effect on adenovirus infection, indicating that this compound has not a global effect on viral entry (Fig. 3B). We also confirmed its inhibitory effect on primary human hepatocytes (PHHs) infected by HCV strain JFH1 (genotype 2a) (Fig. 3C) (20), as well as on 18 different JFH1-based Core-NS2 strain recombinants representing the six HCV major genotypes and important subtypes (Fig. 3D, Table 2) (21–27).

In order to better understand the mechanism of action of SB258585 as an inhibitor of HCV infection, we decided to test another characterized 5-HT6 antagonist, SB399885 which shares a very similar structure (Fig. 3F). The fact that both antagonists inhibit a common step of HCV infection (Fig. 2A, 3G-H) in the absence of their main targeted receptor, modulating PKA activity (Fig.2D) suggests that their common structure of piperazinylbenzenesulfonamides is likely responsible for a common off-target effect.

To better identify the entry step targeted by these compounds, we performed a time-of-addition assay, using proteinase K and bafilomycin A respectively as controls of early and

late step of viral entry. Proteinase K blocks viral internalization through proteolysis of viral particles exposed to the extracellular compartment, while Bafilomycin A blocks the endosomal acidification resulting in the inhibition of viral fusion (28). A comparison of SB258585 and SB399885 to the kinetics of proteinase K and Bafilomycin A treatment rather revealed an inhibition of a late step of the entry process (Fig. 3E, 3I). It is worth noting that the slight difference in the SB258585 curves obtained at 20μM and 100 μM was not statistically significant.

Knowing that CD81-CLDN1 interaction is necessary for clathrin-dependent endocytosis of HCV particles (8), we analyzed the effect of these piperazinylbenzenesulfonamides on CD81-CLDN1 co-localization. A dose-dependent decrease of CD81-CLDN1 co-localization was observed after treatment with SB258585, as confirmed by determining the Pearson correlation coefficient (Fig. 4A-B). Furthermore, we observed a decrease of cell surface CLDN1 expression by flow cytometry analyses in non-infected (Fig. 4C) and infected cells (data not shown) treated with SB258585. This could explain the alteration in CD81-CLDN1 co-localization. The same phenotype was also observed in cells treated with SB399885 (Fig. 4D). Furthermore, kinetic analyses revealed that the decrease of CLDN1 cell surface expression after SB258585 treatment is quite rapid and reversible (Fig. 4E-F). It is worth noting that this compound had no effect on the distribution of other major HCV entry co-receptors, including CD81 (Fig. 5).

Alteration of cell surface expression of CLDN1 mediated by SB258585 is due to CLDN1 intracellular accumulation.

Decreased CLDN1 cell surface expression could be due either to CLDN1 degradation or intracellular accumulation. To answer this question, we first analyzed the total level of CLDN1 by western blot. Treatment of Huh-7 cells with SB258585 and SB399885 did not

affect the amount of CLDN1 (Fig. 4G), indicating that these compounds do not induce CLDN1 degradation. Instead, immunofluorescence analyses showed an intracellular accumulation of CLDN1 in the presence of SB258585 (Fig. 4H), confirmed by an increased co-localization with the intracellular markers TGN46 (Fig.4I), ERGIC53 and GM130 (data not shown). This intracellular accumulation could be due either to an increase in CLDN1 endocytosis or to an alteration in CLDN1 export. To elucidate this, we used an internalization assay based on cell surface biotinylation to determine the kinetics of CLDN1 endocytosis in the presence or absence of the drug. As shown in Fig. 4J, CLDN1 endocytosis was maximal after 1h. The protein amount was comparable in DMSO or SB258585 treated cells, suggesting no alteration of CLDN1 endocytosis. Conversely, at later time points, biotinylated CLDN1 disappeared in DMSO treated cells, suggesting that it had either been degraded or recycled to the cell surface, while it remained stored intracellularly in the presence of the compound. This is in agreement with the accumulation of CLDN1 detected by immunofluorescence (Fig. 4H). Since no change in total CLDN1 level was observed between DMSO and SB258585 treatment (Fig. 4G), it is unlikely that endocytosed CLDN1 is degraded. Rather, CLDN1 must be recycled to the plasma membrane. Accumulation of intracellular CLDN1 observed after SB258585 treatment (Fig. 4H-J) suggests a defect of CLDN1 recycling and explains the decrease of CLDN1 at the cell surface.

PKA inhibition affects HCV late entry step and regulates CLDN1 trafficking.

To further confirm whether SB258585 inhibitory effect on HCV could be mediated by the PKA downstream pathway, we tested the effect of PKA inhibitor H89 on HCV infection. As reported by Farquhar and co-workers (29), we confirmed a dose-dependent inhibitory effect of this compound on both HCVpp and HCVcc of JFH1strain (genotype 2a) at non-toxic concentrations (Fig. 6A-C). We then used a time-of-addition assay with increasing

240 concentrations of H89, and our data indicated an inhibitory effect at a late step of HCV entry
241 (Fig. 6D). Furthermore, as observed for the two piperazinylbenzenesulfonamides, H89
242 treatment also induced a decrease of cell surface expression of CLDN1 (Fig. 6E) without
243 affecting its total level of expression (Fig. 4G), but rather resulting in its intracellular
244 accumulation (Fig. 4H-I). In addition, transfection of an exogenous catalytic subunit of PKA
245 (PRKACA) followed by stimulation of PKA with the activator of adenylyl cyclase forskolin,
246 also increased the phosphorylation level of PKA substrates (Fig. 7A). Interestingly, PKA
247 stimulation caused an increase in cell surface expression of CLDN1 but no increase in
248 CLDN1-CD81 co-localization (Fig. 7B-C). In agreement with this data, no increase in HCV
249 infection was observed after activation of PKA (Fig. 7D).
250 Similar experiments were performed activating the PKA pathway by overexpression
251 of a GPCR, through exogenous transfection of a plasmid encoding 5-HT6 in Huh-7 cells. The
252 increased phosphorylation level of PKA substrates (Fig. 7E), suggested that the exogenous
253 receptor is functional and able to activate the PKA downstream pathway. As observed after
254 PKA transfection, overexpression of 5-HT6 led to an increase in CLDN1 cell surface
255 expression (Fig. 7F), also observed upon SB258585 treatment (Fig. 7G). However, this
256 increase in CLDN1 cell surface localization did not correlate with an increase in CLDN1-
257 CD81 co-localization (Fig. 7H) or HCV infectivity (Fig. 7I).
258 Together, these data strongly suggest that PKA regulates CLDN1 localization at the
259 cell surface. However, its activation does not seem to be sufficient to mediate CLDN1
260 interaction with CD81, which is necessary for HCV entry. Similarly, an increase of CLDN1
261 cell surface expression without modification of CLDN1-CD81 interaction and HCV infection
262 was observed after over-expression of CLDN1 (Fig. 7J-L). The failure in enhancing HCV
263 infection upon CLDN1 overexpression is in accordance with previous data (5). Together,
264 these results suggest that decreasing CLDN1 at plasma membrane strongly impacts HCV

entry, while increasing CLDN1 alone has no effect, probably due to a lack of recruitment to its main partner CD81.

One potential explanation for the failure in increasing CLDN1-CD81 co-localization could be a limited availability of endogenous CD81. To address this hypothesis, we overexpressed this tetraspanin concomitantly with the GPCR 5-HT6. However, no enhancement of HCV infection was observed (Fig. 8A), suggesting that increasing the available quantity of both co-receptors was not sufficient to enhance their interaction and consequently viral entry.

EGFR signaling has been described as important for CLDN1-CD81 interaction (30, 31). To verify if our phenotype was due to an insufficient activation of this receptor and its downstream pathway, we treated Huh-7 with EGF. Although the stimulation induced the phosphorylation of EGFR and thus its activation (Fig. 8B), no enhancement of infectivity, but rather a slight decrease, was observed in our hands after increase of cell surface CLDN1 induced by transfection of 5-HT6 GPCR (Fig. 8C). Therefore, an additional signal upstream of EGFR is likely necessary to relocalize CLDN1 to the site of interaction with CD81.

The C-terminal region of CLDN1 is not involved in PKA-mediated inhibition.

Predicted phosphorylation sites in the cytosolic domains of CLDN1 are only present in the C-terminal region of CLDN1 (32) and could be responsible for its localization. A mutant where the cytosolic C-terminus of CLDN1 was deleted has previously been described to remain functional for HCV entry (5). We therefore used this mutant to determine whether the effect of 5-HT6 activation antagonists is maintained when CLDN1 C-terminus region is deleted. For this, we generated a CRISPR/Cas9 CLDN1 KO cell line (Fig. 9A-B), and we re-expressed a wild type or a C-terminal deleted CLDN1 (Δ Cter) in this cell line (Fig. 9C-D). After verification that the transfection level and the surface localization of the two constructs

were comparable (Fig. 9C), we infected the cells with HCV in the presence or absence of SB258585. As shown in Fig. 9D, the absence of the C-terminus of CLDN1 did not alter the sensitivity of HCV infection to SB258585 or H89, suggesting that CLDN1 C-terminal cytosolic tail is not a direct target for PKA activity and is not required for its recycling.

DISCUSSION

HCV entry is a highly complex multi-step process involving a series of cellular proteins. Trafficking of these entry factors provides an additional level of complexity in the regulation of HCV entry. Here, by screening a chemical compound library, we identified the antagonist of 5-HT6 SB258585 as a novel inhibitor of HCV entry process. This drug, as well as another 5-HT6 antagonist SB399885, with which it shares similarities in structure, inhibits a post-binding step of HCV entry in a 5-HT6 independent manner. These two drugs induced a decrease in recycling of HCV entry co-receptor CLDN1 and its co-localization with CD81. The resulting reduction of CLDN1-CD81 interaction, known to be critical for HCV internalization, likely explains the drop of HCV infectivity. Treatment with these drugs showed a reduction in PKA activity and the involvement of this kinase-related pathway was confirmed to regulate CLDN1 localization and HCV late entry step.

The attempt to detect 5-HT6 in liver biopsies and hepatocytes was unsuccessful. This failure in detecting 5-HT6 mRNA is supported by other reports (33). In addition, SB258585 and SB399885 are supposed to inhibit 5-HT6 in a highly specific way at nanomolar concentrations. Therefore, the fact that in our hands the inhibition is only observed at micromolar concentrations supports the idea of an effect on another target, for which the drug shows less affinity. However, although the major target of these drugs in our model is unlikely to be 5-HT6, these chemical compounds inhibit PKA activity, suggesting an inhibitory effect on one or several other GPCRs likely associated to a Gα stimulatory protein.

315 According to Stitch 5.0 prediction (17), SB258585 shows an affinity for other 5-HT receptors,
316 including the GPCR coupled to Gαs 5-HT7, recently shown to play a role in liver fibrosis
317 (33). Unfortunately no data are available concerning SB399885, although the common
318 structure could suggest similar low-affinity targets.

319 PKA likely controls the export of CLDN1. Indeed, a down-regulation of PKA activity
320 reduces the cell surface expression of CLDN1, whereas its activation shows a direct increase
321 of this tight junction protein at cell surface, confirming a direct correlation between PKA
322 pathway and CLDN1 subcellular localization. The 5-HT6 receptor is a GPCR associated with
323 a G alpha stimulatory protein, known to activate the PKA pathway (34). Therefore, it is not
324 surprising that its overexpression stimulates PKA signaling and the export of the tight
325 junction protein CLDN1, similarly to what happens upon direct PKA transfection or
326 activation. Therefore, this experiment reinforces the hypothesis of a role for GPCRs in
327 regulating PKA signaling in hepatocytes. This is in line with a previous report showing that
328 PKA inhibitors affect HCV entry (29).

329 Activation of the PKA pathway either by forskolin treatment, or by overexpression of
330 the exogenous GPCR 5-HT6, or by overexpression of PKA catalytic subunit itself, increased
331 CLDN1 export at the surface or rescued its surface localization in cells treated with
332 SB258585. However, this was not sufficient to increase the basal level or to rescue HCV
333 infection. Similarly, over-expression of CLDN1 led to an increase in CLDN1 expression at
334 the cell surface without increasing HCV entry. In our case, in addition to analyzing CLDN1
335 expression at the cell surface and HCV infection, we also monitored CD81-CLDN1 co-
336 localization, which was not rescued despite re-export of CLDN1 at the cell surface. Thus,
337 there seems to be a disconnect between the level of CLDN1 expressed at the cell surface and
338 CD81-CLDN1 interaction. These observations are in accordance with Farquhar's work (29),
339 where treatment with forskolin did not enhance HCVcc entry. Since CLDN1 interaction with

the tetraspanin CD81 is necessary to mediate HCV endocytosis (6, 7), this could explain the lack of rescue of HCV infection. The reason why CLDN1-CD81 co-localization is not restored upon PKA activation remains unclear. One possibility could be that in rescue experiments, despite the restoration of cell-surface expression of CLDN1, CD81 is no longer available to interact with CLDN1. The interaction between these two proteins is described to be regulated by the EGF receptor through HRas signaling (30, 31). However, neither overexpression of CD81 concomitantly with the GPCR 5-HT6, nor EGF stimulation restored the phenotype. This suggests that an additional signal upstream of EGFR is needed to target CLDN1 to the site of interaction with CD81. Further investigations are therefore required to better characterize the nature and the dynamics of the interaction between CLDN1 and CD81. However, we cannot exclude that this defect in HCV late entry step is not only due to the decreased interaction between CLDN1 and CD81. In addition to its involvement during exocytosis, there are in fact evidences of a role for cAMP/PKA pathway during endocytosis (reviewed in (35)). Therefore, the defect in HCV entry could not only be associated to CLDN1 localization change, but also to a general perturbation of the membrane trafficking, directly impacting HCV endocytosis. Further investigations are needed in order to elucidate the mechanism connecting PKA pathway activation and endocytosis, necessary to better clarify its additional involvement in HCV entry.

Regulation of CLDN1 trafficking in hepatocytes remains poorly characterized. However, the CLDN1 C-terminal cytosolic tail presents several potential sites of post-translational modification, including phosphorylation and ubiquitination, which could potentially play a role in its trafficking (36). Indeed, other reports indicate a role for the phosphorylation of CLDN1 cytosolic tail in the regulation of its subcellular localization in non-hepatic cells (37–39), or through a competition between phosphorylation and ubiquitination (40), as described for other members of the CLDN family (41, 42). However,

365 in our experimental work, the absence of the C-terminus of CLDN1 did not alter the
366 sensitivity of HCV infection to 5-HT6 and PKA antagonists, excluding a role for a direct
367 phosphorylation on CLDN1. Therefore, an additional, as of yet unidentified, intermediate
368 protein likely phosphorylated by PKA is probably involved in regulation of CLDN1
369 localization in the hepatocyte. However, cAMP/PKA pathway activation has been shown to
370 stimulate exocytosis of several proteins towards both apical and basolateral surface in
371 hepatocytes (reviewed in (35)), suggesting a conserved mechanism of export.

372 Several compounds targeting other GPCRs were identified as HCV inhibitors in our
373 screen. Previous studies described antihistamines, neuroleptic drugs and other ligands of
374 GPCRs as inhibitors of HCV entry (16, 43, 44). In the future it would be interesting to test if
375 the viral resistance mutations against any of these drugs eventually confer cross-resistance to
376 piperazinylbenzenesulfonamides. Moreover, the identification of compounds targeting
377 GPCRs in HCV screens could be in accordance with data from a recent chemical compound
378 screen performed on Ebola and Marburg viruses, identifying the involvement of several
379 antagonists of GPCRs, including 5-HT receptors, as inhibitors of a post-binding step of viral
380 entry (45). In addition, connections between 5-HT receptors and viral infections have already
381 been documented for several viruses, especially post-binding steps of viral entry as for
382 reovirus, JC polyomavirus, chikungunya virus and mouse hepatitis virus (46–49). Several
383 chemical compounds targeting 5-HT receptors were identified as HCV inhibitors in other
384 HCS screens (50, 51). This suggests that a possible common mechanism, potentially affected
385 by drugs targeting 5-HT receptor, might be used by different viruses. In this context, CLDN1
386 might not be the only protein whose trafficking is altered by modulation of 5-HT pathway.
387 Interestingly, in immune cells treated with an inhibitor of 5-HT uptake, HIV entry receptor
388 and co-receptor were also observed to be down-regulated at the cell surface (52); however,
389 the mechanism was not investigated. Further studies are necessary in order to better clarify if

there is actually a common pathway influencing the entry of all these viruses that could represent a potential drug target for wide-range antiviral development.

In summary, we identified SB258585 and SB399885, antagonists of 5-HT6 receptor, as inhibitors of a post-binding step of HCV entry. Although we confirmed the absence of 5-HT6 in liver and hepatic cells, we proved an inhibition of PKA activity as a consequence of the treatment, suggesting an off-target effect of these drugs on another GPCR. We thus confirmed an involvement of PKA in a post-binding step of HCV entry, showing that modulation of PKA activity regulates CLDN1 localization, through regulation of CLDN1 recycling towards the cell surface. We thus suggest a role for PKA in the liver, as a regulator of CLDN1 export, which affects the HCV entry process influencing viruses of the six major genotypes. Finally, our work reinforces the hypothesis of a common pathway shared by several enveloped viruses, involving PKA-dependent signaling in late steps of viral entry.

MATERIAL AND METHODS

Cell culture. Huh-7 and Huh-7.5 cells have been previously described (53, 54) and were cultured at 37°C with 5% CO2 in Dulbecco's modified Eagle's medium (DMEM) supplemented with 10% fetal bovine serum (FBS). Experiments were performed in DMEM supplemented with 5% FBS. Huh-7 and Huh-7.5 cells were authenticated by the company Multiplexion, performing a Multiplex human cell line Authentication Test (MCA) as described at www.multiplexion.de.

For experiments using forskolin and EGF, cells were preincubated during 2h in serum-free medium before incubation with the compound. DMEM, Opti-MEM, phosphate-buffered saline (PBS), goat serum, and FBS were purchased from Life Technologies. PHH were purchased from Biopredic and cultured at 37°C in supplemented Hepatocyte Basal Medium (Clonetics™ HCM™ BulletKit™, Lonza).

Viruses. Cell culture derived HCV **(**HCVcc) were produced by electroporation of Huh-7 cells with *in vitro* transcribed RNA of a modified JFH1 plasmid kindly provided by T. Wakita (National Institute of Infectious Diseases, Tokyo, Japan) (11). This modified JFH1 bears some titer-enhancing mutations and the reconstitution of the A4 epitope in E1 (10). Sequence-confirmed virus stocks of JFH1-based Core-NS2 HCV recombinants were previously generated as described (21–27).

Antibodies. Anti-HCV E1 mouse monoclonal antibody (MAb) A4 was produced *in vitro* using a MiniPerm apparatus (Heraeus) following the manufacturer's protocol. Anti-CD81 MAb (5A6) was kindly provided by S. Levy (Stanford University). Anti-SRB1 antibody C1671 was kindly given by A. Nicosia (OKAIROS, Italy). Anti-CLDN1 (OM 8A9-A3) MAb has been previously described (55). Anti Phospho-(Ser/Thr) PKA Substrate (9621) and anti-HA tag (C29F4) and anti-Phospho-EGFR (Tyr1068)(1H12) mouse mAb (2236) were supplied from Cell Signaling Technology. Anti-EGFR (cocktail R19/48), anti-OCLN (OC-3F10) and anti-CLDN1 (51-9000) were purchased from Life Technologies. Anti-β-tubulin (T5201), anti-HA tag (16B12), anti E-cadherin (AF648), anti-TGN46 (AHP500G), anti-GM130 (610822) and anti-ERGIC53 (ALX-804-602) antibodies were obtained from Sigma, Covance, R&D Systems, AbD Serotec, BD Biosciences and Enzo Life Sciences, respectively. Anti-rat and anti-mouse PE-coupled antibodies were supplied by BD Biosciences. Anti-Mouse Cy3, anti-Mouse Alexa 488, Anti-Rabbit Alexa647, anti-Mouse HRP and anti-Rabbit HRP were purchased from Jackson ImmunoResearch. Goat anti-rat and anti-mouse APC-coupled antibodies as well as anti-goat Alexa488, anti-rat Alexa555, anti-sheep Alexa488 and anti-human Alexa488 coupled antibody were supplied by Life Technologies.

Chemicals. SB258585 hydrochloride (sc-361339), SB399885 hydrochloride (sc-204264), H89 dihydrochloride (sc-3537) and forskolin (sc-3562) were purchased from Santa Cruz

Biotechnology. Bafilomycin A, proteinase K, DAPI and Puromycin dihydrochloride from *Streptomyces alboniger* were obtained from Sigma Aldrich. Mowiol was purchased from Calbiochem. Dimethyl sulfoxide (DMSO), Streptavidin−Agarose beads from *Streptomyces avidinii* and bafilomycin A1 were obtained from Sigma Aldrich. EGF, EZ-link Sulfo-NHS-SS-Biotin, Dynabeads® Sheep Anti-Rat IgG and Hoechst 33342 were purchased from Life Technologies.

Primer list. CLDN1-crispR-F: 5'-CACCGCTTCATTCTCGCCTTCC-3'; CLDN1-crispR-R: 5'-AAACGGAAGGCGAGAATGAAGC-3'; CLDN1-R: 5'-GTGGATCCTCACACGTAGTCTTTCCCGC-3'; CLDN1-F: 5'-TTAAGCTTGCCACCATGGCCAACGCGGGGCTGC-3';
CLDN1-ΔCter-R: 5'-GTGGATCCTCAACAGGAACAGCAAAGTAGGG-3';

Plasmids. pX459-CLDN1 was generated by insertion of the described RNA guides in pSpCas9(BB)-2A-Puro (PX459) (Addgene). pcDNA3.1-CD81-YFP was generated by insertion of YFP sequence in pcDNA3.1-CD81 vector. pCDNA3.1-CLDN1 and pCDNA 3.1-CLDN1 ΔCter were generated by amplification of CLDN1 human cDNA contained in pCMV6-Ac vector (OriGene) by using CLDN1-F and CLDN1-R or CLDN1- ΔCter-R primers respectively and inserted into pCDNA3.1(+) (Invitrogen) by digestion with HindIII and BamH1. HTR6 N-terminus 3xHA-tagged plasmid was purchased from UMR cDNA Resource Center University of Missouri-Rolla (HTR060TN00) and PRKACA ORF mammalian expression plasmid C-HA tag from Sino Biological Inc. (HG11544-CY).

Human biopsies. For mRNA expression analysis of 17 normal tissue samples (Ambion), total RNA (500 ng) was reverse transcribed using SuperScript™ II Reverse Transcriptase (Invitrogen) and random hexamer. Using Taqman gene expression assay (Life Technologies) for 5HT-6 gene (Hs00168381_m1) and RPLP0 (Hs99999902_m1) as control, real-time PCR amplifications were run in duplicate using LightCycler 480 Probe Master (Roche) and were

464 performed on the LightCycler 480 Instrument II (Roche) according to the MIQE guidelines
465 (56). Samples that lacked either a template or reverse transcriptase were used as controls. The
466 relative expression of each gene was calculated according to the 2-ΔCt quantification method
467 where ΔCt value was determined by subtracting the average Ct value of the target gene from
468 the average Ct value of the control gene.
469 **HCS analysis.** 1,120 biologically active compounds from Tocriscreen Total library at 10 mM
470 in pure DMSO were dispensed in 384-well μClear black plates (Greiner bio-one Cat. 781091)
471 using the nanoliter acoustic liquid handler Echo 550® (LabCyte). 16 wells containing pure
472 DMSO were used as controls. Eight hundred Huh-7 cells were seeded in 30 μl in 384-well
473 plates and incubated with each compound respectively at a final concentration of 1, 10 or 20
474 μM at 37°C and 5% CO_2. Sixteen hours later, cells were infected with 30 μl of HCVcc at a
475 MOI of 0.4 and incubated at 37°C and 5% CO_2. After 72 h, 40μl the supernatant was
476 harvested on a second set of 384-well μClear black plates containing twelve hundred Huh-7
477 cells with an automated liquid handler Bravo (Agilent) and incubated at 37°C and 5% CO_2 for
478 48 h. The infected cells in the two sets of 384-well plates were fixed for 30 minutes using
479 formalin solution, neutral buffered, 10% (Sigma-Aldrich, Cat. HT5014) at room temperature.
480 Cells were then permeabilized with 0.1% Triton X-100 in PBS for 3 minutes at room
481 temperature and HCV infected cells were revealed by immunofluorescence with anti-E1
482 antibody (MAb) A4 (1:1000 dilution) for 30 minutes at room temperature. Goat anti-mouse
483 Alexa-488 was used as a secondary antibody (1:500 dilution), while nuclei were labeled with
484 DAPI (1:500 dilution) for 30 minutes at room temperature. Two fields per well were acquired
485 using the 20X objective (NA 0.45) using excitation laser (Ex) at 405 nm and emission filter
486 (Em) at 450 nm for DAPI detection and Ex at 488 nm and Em at 540 nm for virus detection.
487 on an automated confocal microscope InCell 6000 Analyzer (GE Healthcare). Images were
488 analyzed using a dedicated image analysis performed on the Columbus Software allowing

automated quantification of the number of cells and the percentage of infected cells per well. Compounds reducing the cell number by more than 35% compared to the average of DMSO control wells were considered toxic and discarded. Compounds decreasing the percentage of infection of at least 45%, whose effect was confirmed upon re-infection, were identified as positive hits. Image analysis parameters of Columbus software are available upon request.

JFH1 infection assay. JFH1-HCVcc infection was quantified as previously described (10).

Core-NS2 HCV recombinant infection assay. Huh7.5 cells were plated at 7000 cells/well in PDL coated 96 well plates. The following day, four replicates of the described Core-NS2 HCV recombinants were mixed with different concentrations of SB258585 in DMEM supplemented with 10% FBS, along with 8 replicates of virus only without SB258585, and added to Huh7.5 cells for 3 h. Following this incubation, the cells were washed and full medium was added. After a total of 48 h post virus inoculation, the numbers of focus forming units were visualized by HCV-specific immunostaining using NS5A antibody, 9E10 (24). Counting was automated using an ImmunoSpot Series 5 UV Analyzer as described (57) and the counts were normalized to the mean count of virus only.

PHH infection. PHH (Biopredic) were inoculated for 3 h with a cell culture adapted JFH1 strain in the presence of increasing concentrations of SB258585 and infection was measured by quantification of intracellular HCV RNA 24 h post-inoculation, as previously described (20).

HCVpp and infection assays. HCVpp bearing E1E2 glycoproteins of strain JFH1 (genotype 2a) were produced as previously described (58). RD114pp were produced using a plasmid encoding the feline endogenous virus RD114 glycoprotein (59). Huh-7 cells were incubated with pseudotyped particles for 3h at 37°C, concomitantly with increasing concentrations of drugs. At 48h post-infection, firefly luciferase (FLuc) assays were performed following the manufacturer's protocol (Promega).

HCVcc entry assay. After 2 h of JFH1-HCVcc attachment at 4°C, Huh-7 cells were washed and shifted to 37°C to induce viral internalization. Each drug was added every 15 minutes during a 2 h kinetic. Proteinase K (50 µg/ml) and bafilomycin A (25 nM) were included as controls respectively for an early and a late step of viral entry. When treated with proteinase K, cells were washed in cold PBS and incubated with proteinase K for 1 h at 4°C under gentle agitation, before washing them again and adding fresh medium at 37°C. The infection rate was calculated by IF 30 h later and each time point was normalized to the corresponding DMSO condition.

Adenovirus infection. A recombinant adenovirus (AdV) expressing a green fluorescent protein was generated as previously described (10). Huh-7 cells were inoculated with the virus for 2 h at 37°C concomitantly with increasing concentration of SB258585 and cultured for 24 h at 37°C. AdV infections were scored using an Axioplan2 epifluorescence microscope (Zeiss) after fixation and nuclei staining with Hoechst.

Viability assay. Huh-7 cells were incubated for 2 h with increasing concentrations of the indicated compound. A MTS assay was performed 28 h post-treatment, according to the manufacturer's protocol (Promega) in order to evaluate cell viability.

Immunofluorescence and quantification of CLDN1 co-localization with markers of subcellular compartments. Huh-7 cells previously seeded on coverslips were treated with the indicated compounds. After treatment cells were fixed for 30 minutes with 3 % paraformaldehyde. Cells were permeabilized during 5 minutes with 0.1 % Triton X-100 and saturated for 30 minutes with PBS containing 10 % goat serum. Primary antibodies were incubated during 30 minutes in PBS-goat serum. After three washes, secondary antibodies and DAPI were added during 30 minutes. After three more washes, coverslips were mounted on glass slides using Mowiol. Images were taken using a Zeiss-LSM880 or a Zeiss-LSM780 confocal microscope, with a 63X oil objective. Pearson correlation coefficients were

calculated using the Fiji coloc2 plugin on regions of interest (ROIs) from single cells, designed on the basis of cell compartment labeling. Each experiment was repeated at least three times and at least 40 cells for each condition were quantified.

Quantification of CD81-CLDN1 colocalization. Huh-7 cells were seeded on coverslips and treated with the indicated inhibitor. After treatment cells were fixed for 30 minutes with 3 % paraformaldehyde. Cells were incubated for 30 minutes with PBS containing 10 % goat serum. Primary antibodies diluted in PBS-goat serum were added during 30 minutes. After three washes, secondary antibodies and Hoechst were added for another 30 minutes. After three more washes, coverslips were mounted on glass slides using Mowiol. Images were taken using a Zeiss-LSM880 confocal microscope, with a 63X oil objective. Pearson correlation coefficients were calculated using the Fiji coloc2 plugin on regions of interest (ROIs) from single cells, designed on the bases of CD81 surface labeling. Each experiment was repeated at least three times and a total of at least 40 cells for each condition were quantified.

Flow cytometry. Huh-7 cells treated with the indicated compound for the indicated period of time or siRNA transfected Huh-7 cells were incubated for 30 minutes at 4°C with the indicated primary antibody diluted in cold PBS supplemented with 2 % BSA. After three washes with cold PBS-BSA, cells were incubated for 30 minutes at 4°C with secondary antibodies. After three more washes, cells were incubated for another 30 minutes with cold PBS supplemented with 2 mM EDTA and then resuspended and fixed with a formalin solution at a final concentration of 1.5 % formalin. For PKA-HA labeling, cells were permeabilized for 30 minutes with 5% saponin and each following step was performed in the presence of 5% saponin. Cells were analyzed using a BD FACSCANTO II Flow Cytometer. Analyses were performed using Weasel and FlowJo softwares.

Surface biotinylation and endocytosis. Biotinylation assay was performed as previously described (60). A western blot was performed in order to detect CLDN1. Proteins were resolved by SDS-PAGE and transferred on a nitrocellulose membrane. The membrane was immunoblotted with the indicated primary antibody, followed by peroxidase-coupled secondary antibodies. Proteins were detected using a LAS3000 machine (Fuji).

cDNA transfection. Huh-7 cells were seeded in 24-well plates and transfected with 250 ng of DNA using TransIT®-LT1 Transfection Reagent, according to the manufacturer's protocol. Either treatment followed by FACS analyses or infection experiments were performed 48 h post-transfection.

RNA extraction and qRT-PCR. RNA was extracted from Huh-7 cells using the NucleoSpin® RNA extraction kit (Macherey Nagel), and 2 µg were used for cDNA retrotranscription using the High-Capacity cDNA Reverse Transcription Kit (Life Technologies). Taqman® predesigned gene expression assay approach (Applied Biosystems) using a TaqMan FAM-MGB probe (Hs00168381_m1) was used to perform a qPCR in order to quantify HTR6 (50 cycles). RPLP0 (Hs00420895_gH) was used as a housekeeping gene. ΔCt values were calculated according to the formula: Ct(HTR6)-Ct(RPLP0).

CLDN1-KO cell line. Huh-7 cells were seeded in 6-well plates and transfected with 1 µg of pX459-CLDN1 plasmid using the Trans-IT LT1 reagent (Mirus) according to the manufacturer's protocol. Three days after transfection cells were selected using DMEM supplemented with 2 µg/ml of puromycin. Selection was removed after 4 days and cells were cultured in complete DMEM medium. Knocking out was checked both by Western Blotting and flow cytometry analysis. In order to remove the residual population of cells still expressing CLDN1, a selection was performed using Dynabeads® Sheep Anti-Rat IgG after labeling of the cells with anti-CLDN1 OM 8A9-A3 antibody.

Quantification and statistical analysis. Data are presented as means ± standard error of the mean (SEM), except when specified differently. Statistical parameters and analyses are reported in the Fig. legends n represents the number of independent experiments. Where indicated, asterisks denote statistical significance as follows: *p < 0.05 and **p < 0.01, ***p<0.001, ****p<0.0001, ns=non-significant. Statistical analyses were performed using GraphPad Prism 7.

FUNDING INFORMATIONS

This work was supported by the French National Agency for Research on AIDS and Viral Hepatitis (ANRS) and the ANR through ERA-NET Infect-ERA program (ANR-13-IFEC-0002-01). In addition, this study was supported by research grants from the Danish Council for Independent Research–Medical Sciences and the Novo Nordisk Foundation.

ACKNOWLEDGMENTS

We thank F.L. Cosset, C. Rice and T. Wakita for providing essential reagents. We also thank S. Ung for his help in preparing the Fig.s and L. Linna for manuscript proofreading. We are very grateful to A. Danneels for her precious help during the revisions. Immunofluorescence and flow cytometry analyses were performed with the help of the imaging core facility of the BioImaging Center Lille Nord-de-France.

AUTHOR CONTRIBUTION

LR, JD, YR, LC, OS, LL, PB, JP, JB designed the experiments. LR, OS, AV, FH, JP, LF, SB performed the experiments. LR, OS, LL, FH, JP analyzed the results. TFB assisted in study design and contributed reagents. LR, JD wrote the manuscript and all the authors commented on it.

612 **REFERENCES**

613

614 1. Miao Z, Xie Z, Miao J, Ran J, Feng Y, Xia X. 2017. Regulated Entry of Hepatitis C
615 Virus into Hepatocytes. Viruses 9:100.
616 2. Douam F, Lavillette D, Cosset F-L. 2015. The mechanism of HCV entry into host
617 cells. Prog Mol Biol Transl Sci 129:63–107.
618 3. Brazzoli M, Bianchi A, Filippini S, Weiner A, Zhu Q, Pizza M, Crotta S. 2008. CD81
619 is a central regulator of cellular events required for hepatitis C virus infection of human
620 hepatocytes. J Virol 82:8316–8329.
621 4. Potel J, Rassam P, Montpellier C, Kaestner L, Werkmeister E, Tews BA, Couturier
622 C, Popescu C-I, Baumert TF, Rubinstein E, Dubuisson J, Milhiet P-E, Cocquerel L. 2013.
623 EWI-2wint promotes CD81 clustering that abrogates Hepatitis C Virus entry: Dynamics
624 and partitioning of CD81. Cell Microbiol 15:1234–1252.
625 5. Evans MJ, von Hahn T, Tscherne DM, Syder AJ, Panis M, Wolk B, Hatziioannou T,
626 McKeating JA, Bieniasz PD, Rice CM. 2007. Claudin-1 is a hepatitis C virus co-receptor
627 required for a late step in entry. Nature 446:801–805.
628 6. Harris HJ, Farquhar MJ, Mee CJ, Davis C, Reynolds GM, Jennings A, Hu K, Yuan F,
629 Deng H, Hubscher SG, Han JH, Balfe P, McKeating JA. 2008. CD81 and claudin 1
630 coreceptor association: role in hepatitis C virus entry. J Virol 82:5007–5020.
631 7. Harris HJ, Davis C, Mullins JGL, Hu K, Goodall M, Farquhar MJ, Mee CJ, McCaffrey
632 K, Young S, Drummer H, Balfe P, McKeating JA. 2010. Claudin Association with CD81
633 Defines Hepatitis C Virus Entry. J Biol Chem 285:21092–21102.
634 8. Farquhar MJ, Hu K, Harris HJ, Davis C, Brimacombe CL, Fletcher SJ, Baumert TF,
635 Rappoport JZ, Balfe P, McKeating JA. 2012. Hepatitis C virus induces CD81 and claudin-1
636 endocytosis. J Virol 86:4305–4316.
637 9. Ploss A, Evans MJ, Gaysinskaya VA, Panis M, You H, de Jong YP, Rice CM. 2009.
638 Human occludin is a hepatitis C virus entry factor required for infection of mouse cells.
639 Nature 457:882–886.
640 10. Goueslain L, Alsaleh K, Horellou P, Roingeard P, Descamps V, Duverlie G, Ciczora
641 Y, Wychowski C, Dubuisson J, Rouille Y. 2010. Identification of GBF1 as a Cellular Factor
642 Required for Hepatitis C Virus RNA Replication. J Virol 84:773–787.
643 11. Wakita T, Pietschmann T, Kato T, Date T, Miyamoto M, Zhao Z, Murthy K,
644 Habermann A, Krausslich H-G, Mizokami M, Bartenschlager R, Liang TJ. 2005.
645 Production of infectious hepatitis C virus in tissue culture from a cloned viral genome.
646 Nat Med 11:791–796.
647 12. Friesland M, Mingorance L, Chung J, Chisari FV, Gastaminza P. 2013. Sigma-1
648 receptor regulates early steps of viral RNA replication at the onset of hepatitis C virus
649 infection. J Virol 87:6377–6390.
650 13. Hayashida K, Shoji I, Deng L, Jiang D-P, Ide Y-H, Hotta H. 2010. 17beta-estradiol
651 inhibits the production of infectious particles of hepatitis C virus. Microbiol Immunol
652 54:684–690.
653 14. Ishida H, Ohkawa K, Hosui A, Hiramatsu N, Kanto T, Ueda K, Takehara T, Hayashi
654 N. 2004. Involvement of p38 signaling pathway in interferon-alpha-mediated antiviral
655 activity toward hepatitis C virus. Biochem Biophys Res Commun 321:722–727.
656 15. Mannova P, Beretta L. 2005. Activation of the N-Ras-PI3K-Akt-mTOR pathway by
657 hepatitis C virus: control of cell survival and viral replication. J Virol 79:8742–8749.
658 16. Perin PM, Haid S, Brown RJP, Doerrbecker J, Schulze K, Zeilinger C, von Schaewen

659 M, Heller B, Vercauteren K, Luxenburger E, Baktash YM, Vondran FWR, Speerstra S,
660 Awadh A, Mukhtarov F, Schang LM, Kirschning A, Muller R, Guzman CA, Kaderali L,
661 Randall G, Meuleman P, Ploss A, Pietschmann T. 2016. Flunarizine prevents hepatitis C
662 virus membrane fusion in a genotype-dependent manner by targeting the potential
663 fusion peptide within E1. Hepatol Baltim Md 63:49–62.
664 17. Szklarczyk D, Santos A, von Mering C, Jensen LJ, Bork P, Kuhn M. 2016. STITCH 5:
665 augmenting protein-chemical interaction networks with tissue and affinity data. Nucleic
666 Acids Res 44:D380–384.
667 18. Marazziti D, Baroni S, Catena Dell'Osso M, Bordi F, Borsini F. 2011. Serotonin
668 receptors of type 6 (5-HT6): what can we expect from them? Curr Med Chem 18:2783–
669 2790.
670 19. Murray AJ. 2008. Pharmacological PKA inhibition: all may not be what it seems.
671 Sci Signal 1:re4–re4.
672 20. Helle F, Brochot E, Fournier C, Descamps V, Izquierdo L, Hoffmann TW, Morel V,
673 Herpe Y-E, Bengrine A, Belouzard S, Wychowski C, Dubuisson J, Francois C, Regimbeau J-
674 M, Castelain S, Duverlie G. 2013. Permissivity of primary human hepatocytes and
675 different hepatoma cell lines to cell culture adapted hepatitis C virus. PloS One 8:e70809.
676 21. Carlsen THR, Pedersen J, Prentoe JC, Giang E, Keck Z-Y, Mikkelsen LS, Law M,
677 Foung SKH, Bukh J. 2014. Breadth of neutralization and synergy of clinically relevant
678 human monoclonal antibodies against HCV genotypes 1a, 1b, 2a, 2b, 2c, and 3a. Hepatol
679 Baltim Md 60:1551–1562.
680 22. Gottwein JM, Scheel TKH, Jensen TB, Lademann JB, Prentoe JC, Knudsen ML,
681 Hoegh AM, Bukh J. 2009. Development and characterization of hepatitis C virus
682 genotype 1-7 cell culture systems: role of CD81 and scavenger receptor class B type I
683 and effect of antiviral drugs. Hepatol Baltim Md 49:364–377.
684 23. Jensen TB, Gottwein JM, Scheel TKH, Hoegh AM, Eugen-Olsen J, Bukh J. 2008.
685 Highly efficient JFH1-based cell-culture system for hepatitis C virus genotype 5a: failure
686 of homologous neutralizing-antibody treatment to control infection. J Infect Dis
687 198:1756–1765.
688 24. Lindenbach BD, Evans MJ, Syder AJ, Wolk B, Tellinghuisen TL, Liu CC, Maruyama
689 T, Hynes RO, Burton DR, McKeating JA, Rice CM. 2005. Complete replication of hepatitis
690 C virus in cell culture. Science 309:623–626.
691 25. Pedersen J, Carlsen THR, Prentoe J, Ramirez S, Jensen TB, Forns X, Alter H, Foung
692 SKH, Law M, Gottwein J, Weis N, Bukh J. 2013. Neutralization resistance of hepatitis C
693 virus can be overcome by recombinant human monoclonal antibodies. Hepatol Baltim
694 Md 58:1587–1597.
695 26. Scheel TKH, Gottwein JM, Jensen TB, Prentoe JC, Hoegh AM, Alter HJ, Eugen-Olsen
696 J, Bukh J. 2008. Development of JFH1-based cell culture systems for hepatitis C virus
697 genotype 4a and evidence for cross-genotype neutralization. Proc Natl Acad Sci U S A
698 105:997–1002.
699 27. Scheel TKH, Gottwein JM, Carlsen THR, Li Y-P, Jensen TB, Spengler U, Weis N,
700 Bukh J. 2011. Efficient culture adaptation of hepatitis C virus recombinants with
701 genotype-specific core-NS2 by using previously identified mutations. J Virol 85:2891–
702 2906.
703 28. Meertens L, Bertaux C, Dragic T. 2006. Hepatitis C Virus Entry Requires a Critical
704 Postinternalization Step and Delivery to Early Endosomes via Clathrin-Coated Vesicles. J
705 Virol 80:11571–11578.
706 29. Farquhar MJ, Harris HJ, Diskar M, Jones S, Mee CJ, Nielsen SU, Brimacombe CL,
707 Molina S, Toms GL, Maurel P, Howl J, Herberg FW, van Ijzendoorn SCD, Balfe P,

McKeating JA. 2008. Protein kinase A-dependent step(s) in hepatitis C virus entry and infectivity. J Virol 82:8797–8811.
30. Lupberger J, Zeisel MB, Xiao F, Thumann C, Fofana I, Zona L, Davis C, Mee CJ, Turek M, Gorke S, Royer C, Fischer B, Zahid MN, Lavillette D, Fresquet J, Cosset F-L, Rothenberg SM, Pietschmann T, Patel AH, Pessaux P, Doffoël M, Raffelsberger W, Poch O, McKeating JA, Brino L, Baumert TF. 2011. EGFR and EphA2 are host factors for hepatitis C virus entry and possible targets for antiviral therapy. Nat Med 17:589–595.
31. Zona L, Lupberger J, Sidahmed-Adrar N, Thumann C, Harris HJ, Barnes A, Florentin J, Tawar RG, Xiao F, Turek M, Durand SC, Duong FHT, Heim MH, Cosset F-L, Hirsch I, Samuel D, Brino L, Zeisel MB, Le Naour F, McKeating JA, Baumert TF. 2013. HRas signal transduction promotes hepatitis C virus cell entry by triggering assembly of the host tetraspanin receptor complex. Cell Host Microbe 13:302–313.
32. Ahmad W, Shabbiri K, Ijaz B, Asad S, Sarwar MT, Gull S, Kausar H, Fouzia K, Shahid I, Hassan S. 2011. Claudin-1 required for HCV virus entry has high potential for phosphorylation and O-glycosylation. Virol J 8:229.
33. Polat B, Halici Z, Cadirci E, Karakus E, Bayir Y, Albayrak A, Unal D. 2017. Liver 5-HT7 receptors: A novel regulator target of fibrosis and inflammation-induced chronic liver injury in vivo and in vitro. Int Immunopharmacol 43:227–235.
34. Kohen R, Metcalf MA, Khan N, Druck T, Huebner K, Lachowicz JE, Meltzer HY, Sibley DR, Roth BL, Hamblin MW. 1996. Cloning, characterization, and chromosomal localization of a human 5-HT6 serotonin receptor. J Neurochem 66:47–56.
35. Wojtal KA, Hoekstra D, van IJzendoorn SCD. 2008. cAMP-dependent protein kinase A and the dynamics of epithelial cell surface domains: Moving membranes to keep in shape. BioEssays 30:146–155.
36. Offringa R, Huang F. 2013. Phosphorylation-dependent Trafficking of Plasma Membrane Proteins in Animal and Plant Cells: Phosphorylation-dependent Trafficking of Plasma Membrane Proteins. J Integr Plant Biol 55:789–808.
37. French AD, Fiori JL, Camilli TC, Leotlela PD, O'Connell MP, Frank BP, Subaran S, Indig FE, Taub DD, Weeraratna AT. 2009. PKC and PKA phosphorylation affect the subcellular localization of claudin-1 in melanoma cells. Int J Med Sci 6:93–101.
38. Fujibe M, Chiba H, Kojima T, Soma T, Wada T, Yamashita T, Sawada N. 2004. Thr203 of claudin-1, a putative phosphorylation site for MAP kinase, is required to promote the barrier function of tight junctions. Exp Cell Res 295:36–47.
39. Jian Y, Chen C, Li B, Tian X. 2015. Delocalized Claudin-1 promotes metastasis of human osteosarcoma cells. Biochem Biophys Res Commun 466:356–361.
40. Shiomi R, Shigetomi K, Inai T, Sakai M, Ikenouchi J. 2015. CaMKII regulates the strength of the epithelial barrier. Sci Rep 5:13262.
41. Ikari A. 2006. Phosphorylation of paracellin-1 at Ser217 by protein kinase A is essential for localization in tight junctions. J Cell Sci 119:1781–1789.
42. Takahashi S, Iwamoto N, Sasaki H, Ohashi M, Oda Y, Tsukita S, Furuse M. 2009. The E3 ubiquitin ligase LNX1p80 promotes the removal of claudins from tight junctions in MDCK cells. J Cell Sci 122:985–994.
43. He S, Lin B, Chu V, Hu Z, Hu X, Xiao J, Wang AQ, Schweitzer CJ, Li Q, Imamura M, Hiraga N, Southall N, Ferrer M, Zheng W, Chayama K, Marugan JJ, Liang TJ. 2015. Repurposing of the antihistamine chlorcyclizine and related compounds for treatment of hepatitis C virus infection. Sci Transl Med 7:282ra49–282ra49.
44. Hu Z, Hu X, He S, Yim HJ, Xiao J, Swaroop M, Tanega C, Zhang Y, Yi G, Kao CC, Marugan J, Ferrer M, Zheng W, Southall N, Liang TJ. 2015. Identification of novel anti-hepatitis C virus agents by a quantitative high throughput screen in a cell-based

757 infection assay. Antiviral Res 124:20–29.
758 45. Cheng H, Lear-Rooney CM, Johansen L, Varhegyi E, Chen ZW, Olinger GG, Rong L.
759 2015. Inhibition of Ebola and Marburg Virus Entry by G Protein-Coupled Receptor
760 Antagonists. J Virol 89:9932–9938.
761 46. Assetta B, Maginnis MS, Gracia Ahufinger I, Haley SA, Gee GV, Nelson CDS, O'Hara
762 BA, Allen Ramdial S -a. A, Atwood WJ. 2013. 5-HT2 Receptors Facilitate JC Polyomavirus
763 Entry. J Virol 87:13490–13498.
764 47. Bialowas S, Hagbom M, Nordgren J, Karlsson T, Sharma S, Magnusson K-E,
765 Svensson L. 2016. Rotavirus and serotonin cross-talk in diarrhoea. PLoS One
766 11:e0159660.
767 48. Elphick GF, Querbes W, Jordan JA, Gee GV, Eash S, Manley K, Dugan A, Stanifer M,
768 Bhatnagar A, Kroeze WK, Roth BL, Atwood WJ. 2004. The human polyomavirus, JCV, uses
769 serotonin receptors to infect cells. Science 306:1380–1383.
770 49. Mainou BA, Ashbrook AW, Smith EC, Dorset DC, Denison MR, Dermody TS. 2015.
771 Serotonin Receptor Agonist 5-Nonyloxytryptamine Alters the Kinetics of Reovirus Cell
772 Entry. J Virol 89:8701–8712.
773 50. Hu Z, Lan K-H, He S, Swaroop M, Hu X, Southall N, Zheng W, Liang TJ. 2014. Novel
774 Cell-Based Hepatitis C Virus Infection Assay for Quantitative High-Throughput Screening
775 of Anti-Hepatitis C Virus Compounds. Antimicrob Agents Chemother 58:995–1004.
776 51. Chockalingam K, Simeon RL, Rice CM, Chen Z. 2010. A cell protection screen
777 reveals potent inhibitors of multiple stages of the hepatitis C virus life cycle. Proc Natl
778 Acad Sci 107:3764–3769.
779 52. Greeson JM, Gettes DR, Spitsin S, Dubé B, Benton TD, Lynch KG, Douglas SD, Evans
780 DL. 2016. The Selective Serotonin Reuptake Inhibitor Citalopram Decreases Human
781 Immunodeficiency Virus Receptor and Coreceptor Expression in Immune Cells. Biol
782 Psychiatry 80:33–39.
783 53. Blight KJ, Kolykhalov AA, Rice CM. 2000. Efficient initiation of HCV RNA
784 replication in cell culture. Science 290:1972–1974.
785 54. Nakabayashi H, Taketa K, Miyano K, Yamane T, Sato J. 1982. Growth of human
786 hepatoma cells lines with differentiated functions in chemically defined medium. Cancer
787 Res 42:3858–3863.
788 55. Fofana I, Krieger SE, Grunert F, Glauben S, Xiao F, Fafi-Kremer S, Soulier E, Royer
789 C, Thumann C, Mee CJ, McKeating JA, Dragic T, Pessaux P, Stoll-Keller F, Schuster C,
790 Thompson J, Baumert TF. 2010. Monoclonal anti-claudin 1 antibodies prevent hepatitis
791 C virus infection of primary human hepatocytes. Gastroenterology 139:953–964,
792 964.e1–4.
793 56. Bustin SA, Benes V, Garson JA, Hellemans J, Huggett J, Kubista M, Mueller R, Nolan
794 T, Pfaffl MW, Shipley GL, Vandesompele J, Wittwer CT. 2009. The MIQE Guidelines:
795 Minimum Information for Publication of Quantitative Real-Time PCR Experiments. Clin
796 Chem 55:611–622.
797 57. Gottwein JM, Scheel TKH, Callendret B, Li Y-P, Eccleston HB, Engle RE,
798 Govindarajan S, Satterfield W, Purcell RH, Walker CM, Bukh J. 2010. Novel infectious
799 cDNA clones of hepatitis C virus genotype 3a (strain S52) and 4a (strain ED43): genetic
800 analyses and in vivo pathogenesis studies. J Virol 84:5277–5293.
801 58. Bartosch B, Dubuisson J, Cosset F-L. 2003. Infectious hepatitis C virus pseudo-
802 particles containing functional E1-E2 envelope protein complexes. J Exp Med 197:633–
803 642.
804 59. Sandrin V, Boson B, Salmon P, Gay W, Negre D, Le Grand R, Trono D, Cosset F-L.
805 2002. Lentiviral vectors pseudotyped with a modified RD114 envelope glycoprotein

show increased stability in sera and augmented transduction of primary lymphocytes and CD34+ cells derived from human and nonhuman primates. Blood 100:823–832.
60. Belouzard S, Delcroix D, Rouille Y. 2004. Low levels of expression of leptin receptor at the cell surface result from constitutive endocytosis and intracellular retention in the biosynthetic pathway. J Biol Chem 279:28499–28508.

FIGURE LEGENDS

Figure 1: Identification of the 5-HT6 antagonist SB258585 as a new inhibitor of the HCV life cycle. (A-C) A HCS screen with a library of 1120 chemical compounds was performed at three different concentrations (1 μM, 10 μM and 20 μM). Dot-plots show the distributions of the populations on the bases of cell number and percentage of HCVcc JFH1 (genotype 2a) infected cells at the indicated concentrations. Each dot represents one compound. Green lines represent the average values corresponding to DMSO control wells. Red lines represent the selected cut-offs, determining the positive hits (light red squares). (D) Summary of the positive hits selected according to the cut-offs, at each concentration. The red circle indicates compounds confirmed as positive hits for at least two concentrations. (E) Graph showing the percentage of HCVcc infection corresponding to the wells treated with chemical compounds targeting in a more or less specific way 5-HT6, normalized to the mean of the DMSO control wells at each concentration. The green line corresponds to the compound SB258585 hydrochloride. (F) Wells corresponding to DMSO and SB258585 for each concentration of the screen. Nuclei are shown in blue, HCV E1 staining in green.

Figure 2: SB258585 inhibits HCV infection, modulating PKA in a 5-HT6 independent manner. (A) Huh-7 cells were treated with SB258585 at different concentrations for 2 h prior, during or after JFH1 HCVcc incubation, following the kinetics schematized. Infection was quantified at 30 h post-infection by immunofluorescence. (B) Huh-7 cells were treated

with the drug 2 h, followed by 28 h of rest. A MTS assay was performed in order to evaluate the cell toxicity. (C) Quantification of 5-HT6 mRNA level by qRT-PCR in 17 tissues from human biopsies. (D) Huh-7 cells were treated for 2 h with DMSO, H89 (10 μM), SB258585 (100 μM) or SB399885 (100 μM). A representative western blot from n=3 and relative quantification of total phosphorylation of PKA substrates normalized to the loading control β-tubulin are presented. Results are presented as means ± standard error of the mean (SEM) for n=3 (A, B, D). One-way (B, D) or Two-way ANOVA (A) respectively followed by Dunnett or Bonferroni post-test were performed as statistical tests. *, $P < 0.05$; **, $P < 0.01$; ***, $P < 0.001$; ****, $P < 0.001$.

Figure 3: Piperazinylbenzenesulfonamides inhibit a late step of HCV entry in all the major genotypes. (A) Huh-7 cells were treated for 3 h with SB258585 at different concentrations concomitantly with JFH1 HCVpp or RD114pp incubation. At 48 h post-infection, cells were lysed and luciferase activity was measured in order to quantify the infection. (B) Huh-7 cells were incubated for 2 h with SB258585 at different concentrations along with GFP-Adenovirus. The percentage of infection was determined by quantifying GFP-positive cells at 24 h post-infection. (C) Primary human hepatocytes (PHHs) were treated for 2 h with SB258585 at different concentrations, in addition to JFH1 HCVcc. Infection was quantified by RTqPCR at 24 h post-infection. (D) Huh-7.5 cells were treated for 3 h with SB258585 in addition to JFH1-based HCV genotype 1-6 recombinant viruses with strain specific core-NS2. Infection was quantified by immunofluorescence at 48 h post-inoculation. Error bars represent SD. (E) After 1 h of viral attachment at 4°C, Huh-7 cells were shifted at 37°C and treated with SB258585 at the indicated concentrations, following 15-minute kinetics during 2 h. Proteinase K (50 μg/ml) and bafilomycin A (25 nM) were used as controls respectively for early and late entry steps. Infection was quantified at 30 h post-

infection by immunofluorescence and each time point was normalized to the corresponding DMSO condition. (F) Chemical structure of SB258585 and SB399885. (G) Huh-7 cells were treated with SB399885 at different concentrations for 2 h prior, during or after JFH1 HCVcc incubation, following the kinetics schematized. Infection was quantified at 30 h post-infection by immunofluorescence. (H) Huh-7 cells were treated with SB399885 2 h, followed by 28 h of resting. A MTS assay was performed in order to evaluate the cell toxicity. (I) After 1 h of viral attachment at 4°C, Huh-7 cells were shifted at 37°C and treated with SB399885 at the indicated concentration, following 15-minute kinetics during 2 h. Proteinase K (50 µg/ml) and bafilomycin A (25 nM) were used as controls respectively for early and late entry steps. Infection was quantified at 30 h post-infection by immunofluorescence and each time point was normalized to the corresponding DMSO condition. Results are presented as means ± standard error of the mean (SEM) for n=3 (A-D, G-H) and n=2 (E, I). PHH results are presented as mean of triplicates ± SEM for two independent experiments. One-way (B, C, H) or Two-way ANOVA (A, G) respectively followed by Dunnett or Bonferroni post-test were performed as statistical tests. *, $P < 0.05$; **, $P < 0.01$; ***, $P < 0.001$; ****, $P < 0.001$; *ns*, non significant.

Figure 4: SB258585 alters CLDN1 recycling causing its intracellular accumulation. (A) Huh-7 cells were treated for 2 h with DMSO or increasing concentrations of SB258585. Cell surface expression of CD81 and CLDN1 was analyzed by immunofluorescence. Images were taken using a Zeiss LSM-880 and 63X objective. (B) Pearson correlation coefficient (PCC) was calculated on cell surface ROIs from at least 40 different cells in each condition. (C) Huh-7 cells were treated for two hours with DMSO or increasing concentrations of SB258585 and CLDN1 expression was analysed by flow cytometry. Curves from a representative experiment are shown. Mean fluorescent intensities relative to the DMSO-treated condition

are also presented. (D) Huh-7 cells were treated for two hours with DMSO or increasing concentrations of SB399885 and CLDN1 expression was analyzed by flow cytometry. (E) Huh-7 cells were incubated for the indicated periods with SB258585 (100 µM). CLDN1 present at the cell surface was quantified by flow cytometry. (F) Huh-7 cells were treated for 2 h with SB258585 (100 µM). The drug was then removed and replaced by DMEM for the indicated time. Cytometry analyses were performed to quantify CLDN1 at cell surface. Mean fluorescence intensities relative to the DMSO-treated condition are shown (D-F). (G) Huh-7 cells were treated for 2 h with DMSO, SB258585 (100 µM), SB399885 (100 µM) or H89 (10 µM). The total quantity of CLDN1 was assessed by Western Blot. β-tubulin was used as a loading control. (H) Huh-7 cells were treated for 2 h with DMSO, SB258585 (100 µM), or H89 (10 µM). CLDN1 subcellular localization was determined by immunofluorescence after membrane permeabilization. Images were taken at 63X objective. (I) TGN46 was stained concomitantly with CLDN1 and PCCs were calculated for intracellular CLDN1-TGN46 co-localization for n>35 cells for each condition. (J) After surface biotinylation, Huh-7 cells were incubated at 37°C with DMSO or SB258585 (100 µM) for the indicated time. Biotin remaining at the cell surface was cleaved using glutathione. The amount of internalized CLDN1 was determined by western blotting after pull-down of biotin-labeled proteins with streptavidin-agarose beads. A representative western blot from n=3 is presented. All results are presented as means ± standard error of the mean (SEM) for n=3. One-way ANOVA (B-E, I) or Two-way ANOVA (F) respectively followed by Dunnett or Bonferroni post-test were performed as statistical tests. *, $P < 0.05$; **, $P < 0.01$; ***, $P < 0.001$; ****, $P < 0.001$. Scale bars = 30 µm.

Figure 5: SB258585 does not alter the surface localization of the other main HCV entry factors. (A) Huh-7 cells were treated for two hours with DMSO or increasing concentrations

908 of SB258585. A surface biotinylation followed by a biotin immunoprecipitation was
909 performed and a representative western blot against OCLN is shown. The quantity of
910 biotinylated OCLN was determined using Fiji from western blots corresponding to n=3. (B-E)
911 Huh-7 cells were treated for 2 h with DMSO or increasing concentrations of SB258585.
912 CD81 (B), EGFR (C), SRB1 (D) and E-cadherin (E) expression were analyzed by flow
913 cytometry. Curves from a representative experiment are shown. Mean fluorescence intensities
914 relative to the DMSO-treated condition are presented as means ± SEM. All the results are
915 presented as means ± SEM for n=3. One-way ANOVA followed by Dunnett post-test were
916 performed as statistical tests. *ns*, non significant.
917
918 **Figure 6: Inhibition of PKA signaling pathway down-regulates HCV entry and CLDN1**
919 **cell surface localization.** (A) Huh-7 cells were treated 2 h with H89 at different
920 concentrations. An MTS assay was performed 30 h post treatment in order to evaluate the cell
921 toxicity of the compound. (B) Huh-7 cells were treated for 3 h with H89 at different
922 concentrations along with JFH1 HCVpp and RD114pp. At 48 h post-infection, cells were
923 lysed and luciferase activity was measured in order to quantify the infection. (C) Huh-7 cells
924 were treated with H89 at different concentrations in accordance with the kinetics schematized,
925 along with JFH1 HCVcc. Infection was quantified at 30 h post-infection by
926 immunofluorescence. (D) After 1 h of viral attachment at 4°C, Huh-7 cells were shifted at
927 37°C and treated with H89 (10 µM), following 15-minute kinetics during 2 h. Proteinase K
928 (50 µg/ml) and bafilomycin A (25 nM) were used as controls respectively for early and late
929 entry steps. Infection was quantified at 30 h post-infection by immunofluorescence and each
930 time point was normalized to the corresponding DMSO condition. (E) Huh-7 cells were
931 treated for 2 h with DMSO or H89 (10 µM). Cell surface CLDN1 was analyzed by flow
932 cytometry. Curves from a representative experiment and mean fluorescence intensities

933 relative to the DMSO-treated condition are shown. Results are presented as means ± SEM for
934 n=3 (A-C, E) and n=2 (D). Two-tailed Student's T test (E), One-way (A) or Two-way
935 ANOVA (B-C) respectively followed by Dunnett or Bonferroni post-test were performed as
936 statistical tests. *, $P < 0.05$; **, $P < 0.01$; ***, $P < 0.001$; ****, $P < 0.001$.
937
938 **Figure 7: PKA activation increases CLDN1 localization at cell surface, without**
939 **increasing HCV entry or CLDN1-CD81 co-localization.** (A-D) Huh-7 cells were
940 transfected with pcDNA or pcDNA-PRKACA for 48 h. Cells were treated for 2 h with
941 DMSO, forskolin (20 μM) as indicated. (A) A representative western blot from n=3 is
942 presented, in order to analyse the phosphorylation of PKA substrates. β-tubulin was used as a
943 loading control and PKA transfection was checked by HA immuno-blotting. (B) Cytometry
944 analysis was performed for quantifying CLDN1 cell surface localization and PKA-HA
945 transfection. Mean fluorescence intensities relative to the DMSO-treated condition from n=3
946 are shown. (C) CLDN1 and CD81 were analyzed by immunofluorescence and PCCs were
947 calculated after confocal image acquisition on cell surface ROIs from at least 40 different
948 cells in each condition. (D) Transfected cells were treated for 2 h with DMSO or forskolin (20
949 μM), together with HCVcc. Infection was quantified at 30h post-infection by
950 immunofluorescence. (E-I) Huh-7 cells were transfected for 48 h with pcDNA or pcDNA-5-
951 HT6. (E) A representative western blot from n=2 and relative quantification of total
952 phosphorylation of PKA substrates normalized to the loading control β-tubulin are presented.
953 HA-5-HT6 transfection was checked by HA immuno-blotting. (F-G). Cell surface CLDN1
954 and HA-5-HT6 were immunolabeled and quantified by flow cytometry. Mean fluorescence
955 intensities relative to the DMSO-treated condition are shown. (G) Transfected Huh-7 cells
956 were treated 2 h with SB258585 (100 μM) before labeling for flow cytometry analyses. (H)
957 CLDN1 and CD81 immunostaining followed by confocal microscopy allowed for the

calculation of PCCs on cell surface ROIs from at least 40 different cells in each condition. (I) Transfected Huh-7 cells were infected 2h with HCVcc. Infection was quantified at 30 h post-infection by immunofluorescence. (J-L) Huh-7 cells were transfected for 48 h with pcDNA or pcDNA-CLDN1. Cell surface CLDN1 was immunolabeled and quantified by flow cytometry. Mean fluorescence intensities relative to the DMSO-treated condition are shown (J). CLDN1 and CD81 immunostaining followed by confocal microscopy allowed for the calculation of PCCs on cell surface ROIs from at least 40 different cells in each condition (K). Transfected cells were infected with HCVcc 48 h post-transfection. Infection was quantified at 30 h post-infection by immunofluorescence (L). Results are presented as means ± SEM for n=3 (C-D, H-I) or n=4 (B, F-G, J-L) independent experiments. Two-tailed Student's T test (E-F, H-L) or Two-way ANOVA (B-D, G) followed by Bonferroni post-test were performed as statistical tests. *, $P < 0.05$; ***, $P < 0.001$; *ns*, non significant.

Figure 8: Increase of CLDN1 localization at cell surface is not sufficient to increase HCV entry, neither upon CD81 over-expression nor EGF stimulation. (A) Huh-7 cells were transfected with pcDNA, HA-5-HT6, CD81-YFP alone or in combination as indicated. 48 h post-transfection cells were infected with JFH1-HCVcc. 30 hpi cells were fixed and infection rate was determined by IF. (B) After 2 h of starvation, Huh-7 cells were non-stimulated or stimulated 1 h with EGF (1 μg/ml). A western blot was performed to verify the activation of EGFR, through phosphorylation. β-tubulin was used as a loading control. (C) Huh-7 cells transfected 48 h with pcDNA, HA-5-HT6, CD81-YFP alone or in combination, after 2 h of starvation, were treated 1 h with EGF (1 μg/ml) and infected 2 h with JFH1-HCVcc concomitantly with EGF (1 μg/ml). 30 hpi cells were fixed and infection rate was determined by IF. Results are presented as means ± SEM for n=2 (A, C). One-way (A) or Two-way

ANOVA (C) respectively followed by Dunnett or Bonferroni post-test were performed as statistical tests. *ns*, non significant.

Figure 9: Deletion of CLDN1 C-terminal region does not alter HCV sensitivity to SB258585 and H89. (A-D) Flow cytometry (A) and western blot (B) were performed on CLDN1 CrispR/CAS9 and control pX459 cells, in order to evaluate CLDN1 silencing. OCLN was used as a loading control for the western blot. (C-D) CLDN1 CrispR/CAS9 cells were transfected respectively with pcDNA 3.1, CLDN1 WT or ΔCter. 48 h post-transfection cells were labeled for CLDN1 at the cell surface and analyzed by flow cytometry (C) or infected with JFH1-HCVcc (D). 30 hpi cells were fixed and infection rate was determined by IF. Results are presented as means ± SEM for n=3. Two-way ANOVA (D) followed by Bonferroni post-test was performed as statistical tests. ****, $P < 0.001$.

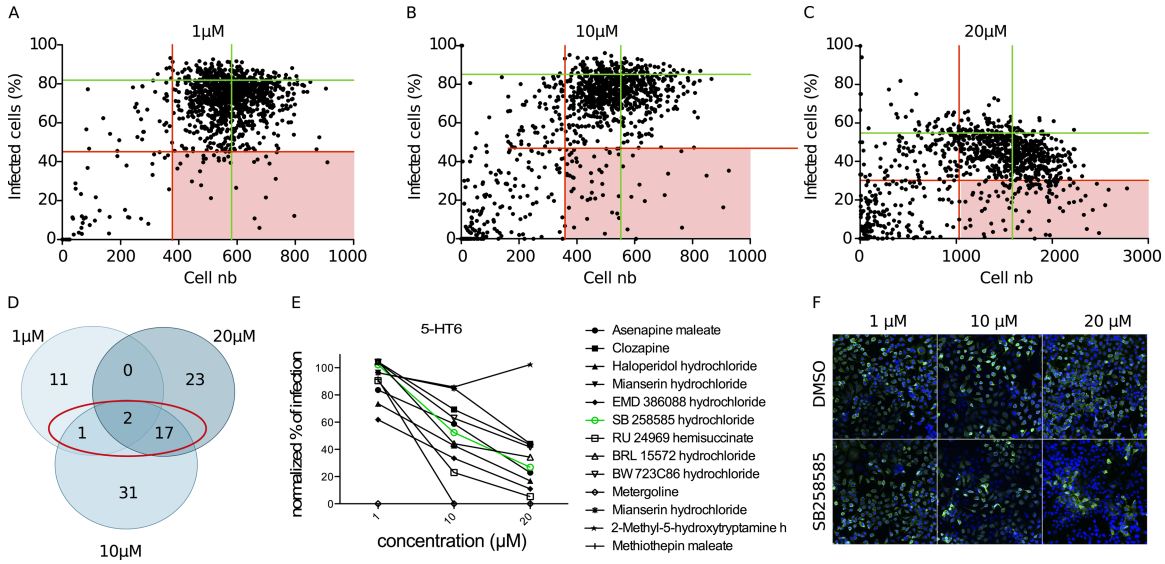
A
1µM
Infected cells (%)
Cell nb
B
10µM
Infected cells (%)
Cell nb
C
20µM
Infected cells (%)
Cell nb
D
1µM
20µM
10µM
11
0
23
2
1
17
31
E
5-HT6
normalized %of infection
concentration (µM)
Asenapine maleate
Clozapine
Haloperidol hydrochloride
Mianserin hydrochloride
EMD 386088 hydrochloride
SB 258585 hydrochloride
RU 24969 hemisuccinate
BRL 15572 hydrochloride
BW 723C86 hydrochloride
Metergoline
Mianserin hydrochloride
2-Methyl-5-hydroxytryptamine h
Methiothepin maleate
F
1 µM
10 µM
20 µM
DMSO
SB258585

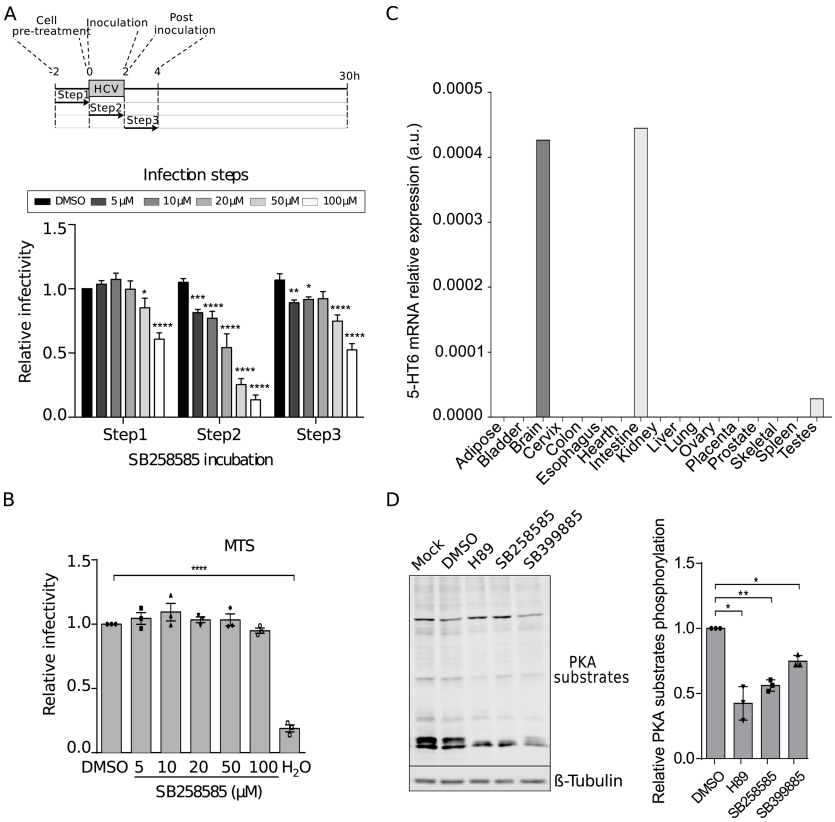
A
Cell pre-treatment
Inoculation
Post inoculation
-2
0
2
4
30h
HCV
Step1
Step2
Step3
Infection steps
DMSO
5 µM
10 µM
20 µM
50 µM
100 µM
Relative infectivity
1.5
1.0
0.5
0.0
Step1
Step2
Step3
SB258585 incubation
C
5-HT6 mRNA relative expression (a.u.)
0.0005
0.0004
0.0003
0.0002
0.0001
0.0000
Adipose
Bladder
Brain
Cervix
Colon
Esophagus
Hearth
Intestine
Kidney
Liver
Lung
Ovary
Placenta
Prostate
Skeletal
Spleen
Testes
B
MTS
Relative infectivity
1.5
1.0
0.5
0.0
DMSO
5
10
20
50
100
H2O
SB258585 (µM)
D
Mock
DMSO
H89
SB258585
SB399885
PKA substrates
ß-Tubulin
Relative PKA substrates phosphorylation
1.5
1.0
0.5
0.0
DMSO
H89
SB258585
SB399885

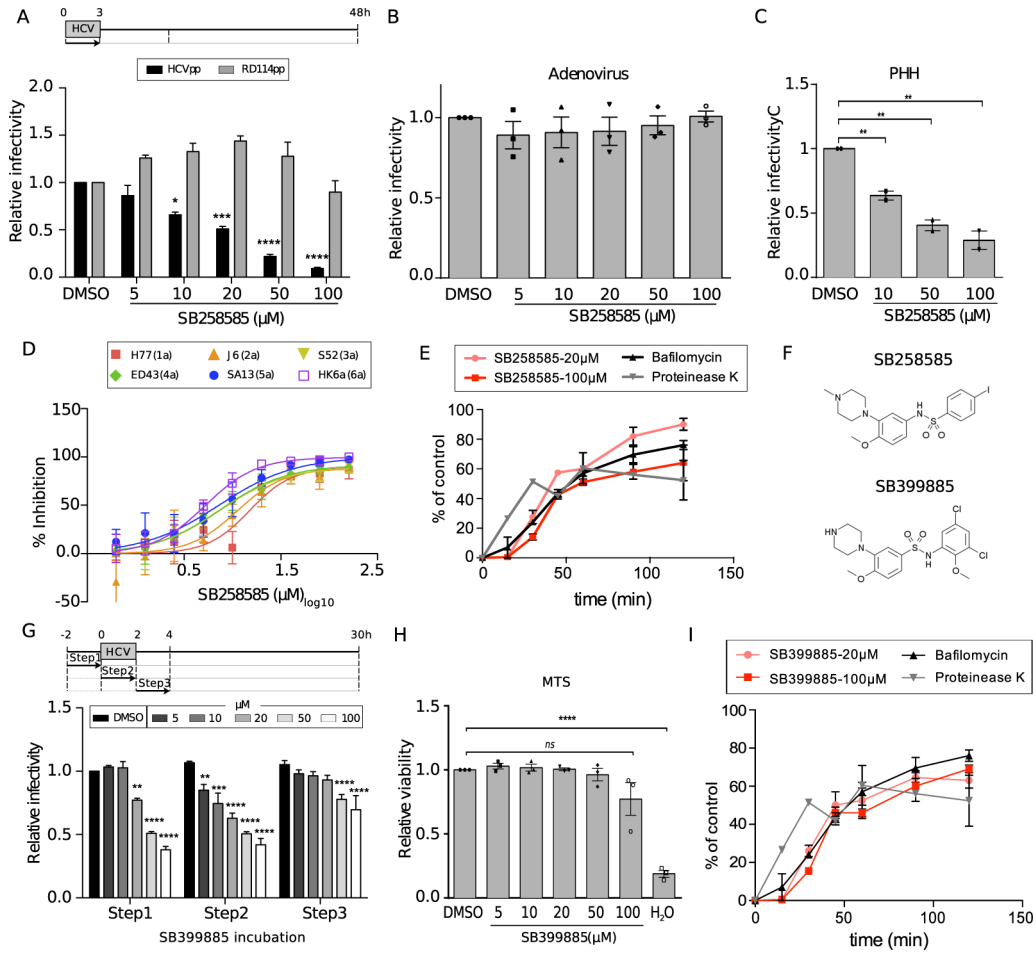
A
0
3
48h
HCV
HCVpp
RD114pp
Relative infectivity
DMSO
5
10
20
50
100
SB258585 (μM)
B
Adenovirus
Relative infectivity
SB258585 (μM)
C
PHH
Relative infectivityC
SB258585 (μM)
D
H77 (1a)
J 6 (2a)
S52 (3a)
ED43 (4a)
SA13 (5a)
HK6a (6a)
% Inhibition
SB258585 (μM)log10
E
SB258585-20μM
SB258585-100μM
Bafilomycin
Proteinease K
% of control
time (min)
F
SB258585
SB399885
G
-2
0
2
4
30h
Step1
Step2
Step3
HCV
μM
DMSO
5
10
20
50
100
Relative infectivity
SB399885 incubation
H
MTS
Relative viability
ns
DMSO
5
10
20
50
100
H2O
SB399885(μM)
I
SB399885-20μM
SB399885-100μM
Bafilomycin
Proteinease K
% of control
time (min)

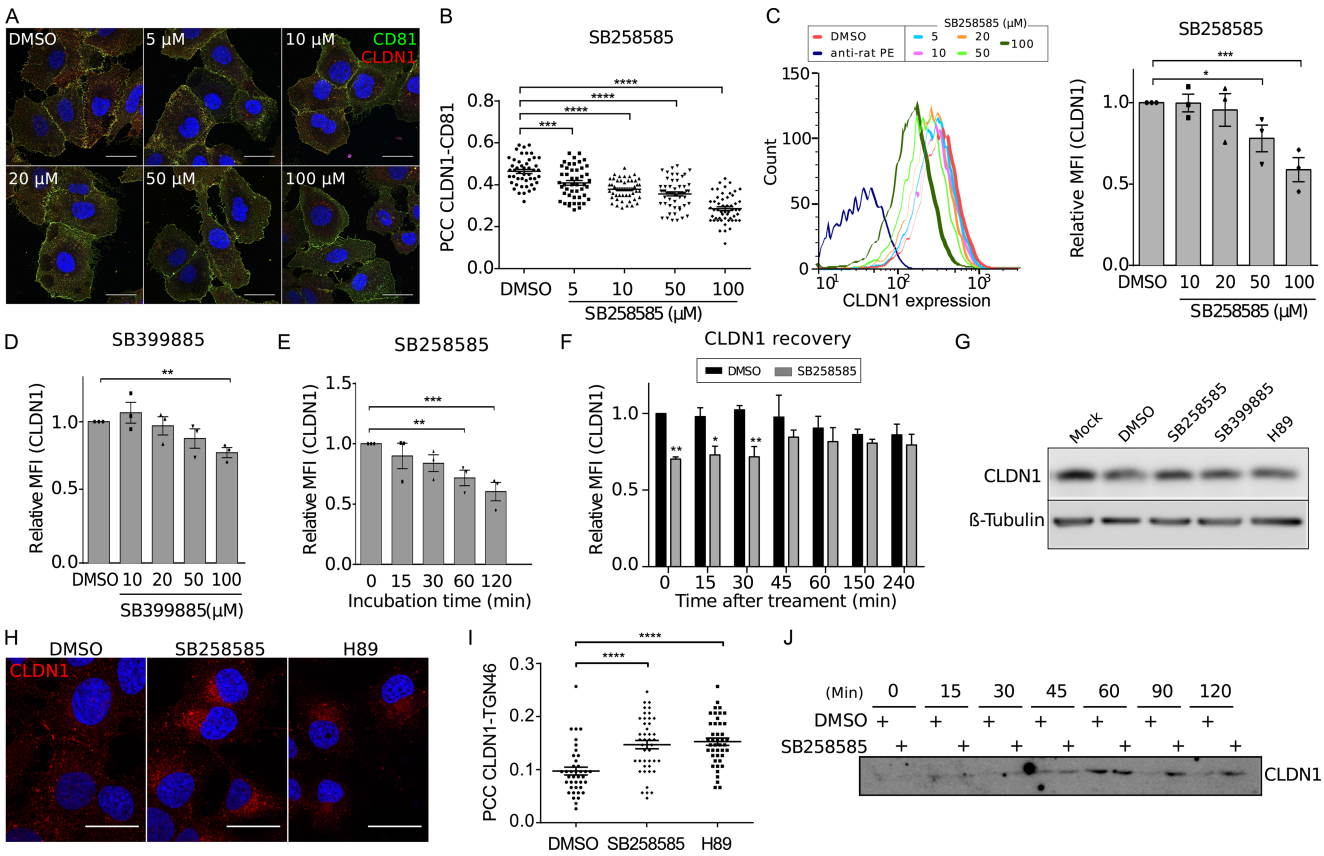
A
DMSO
5 μM
10 μM
CD81
CLDN1
20 μM
50 μM
100 μM
B
SB258585
PCC CLDN1-CD81
DMSO 5 10 50 100
SB258585 (μM)
C
SB258585 (μM)
DMSO
anti-rat PE
5 10 20 50 100
Count
CLDN1 expression
SB258585
Relative MFI (CLDN1)
DMSO 10 20 50 100
SB258585 (μM)
D
SB399885
Relative MFI (CLDN1)
DMSO 10 20 50 100
SB399885(μM)
E
SB258585
Relative MFI (CLDN1)
0 15 30 60 120
Incubation time (min)
F
CLDN1 recovery
DMSO
SB258585
Relative MFI (CLDN1)
0 15 30 45 60 150 240
Time after treament (min)
G
Mock
DMSO
SB258585
SB399885
H89
CLDN1
ß-Tubulin
H
DMSO
SB258585
H89
CLDN1
I
PCC CLDN1-TGN46
DMSO SB258585 H89
J
(Min) 0 15 30 45 60 90 120
DMSO + + + + + + +
SB258585 + + + + + + +
CLDN1

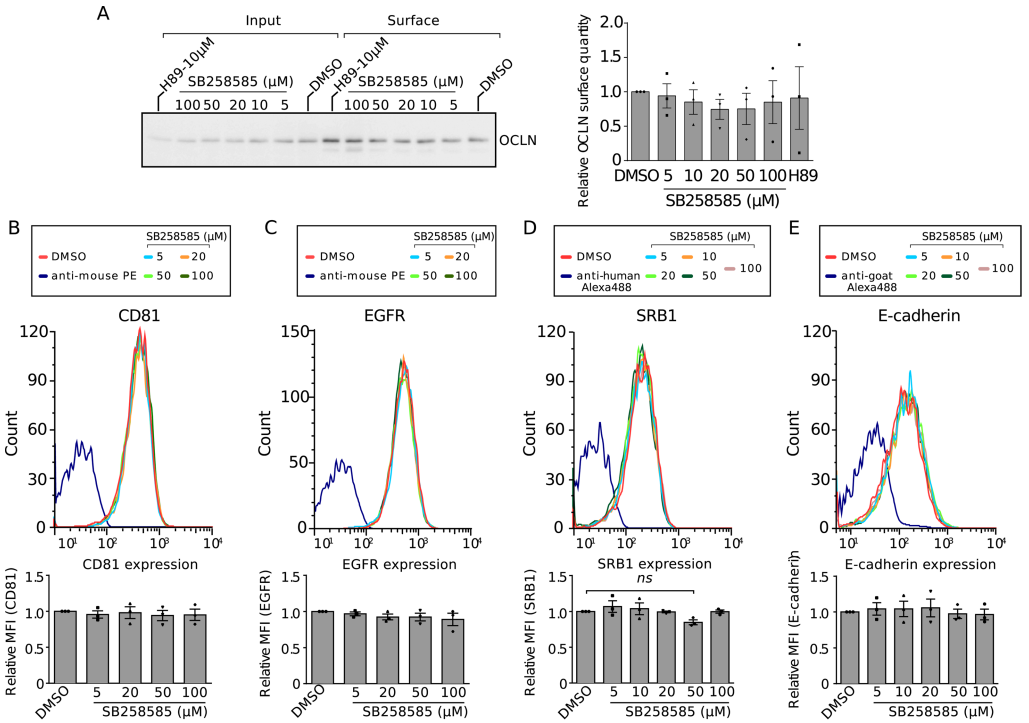
A
Input
Surface
H89-10μM
SB258585 (μM)
DMSO
100 50 20 10 5
OCLN
Relative OCLN surface quantity
DMSO 5 10 20 50 100 H89
SB258585 (μM)
B
C
D
E
DMSO
anti-mouse PE
anti-human Alexa488
anti-goat Alexa488
CD81
EGFR
SRB1
E-cadherin
Count
CD81 expression
EGFR expression
SRB1 expression
E-cadherin expression
Relative MFI (CD81)
Relative MFI (EGFR)
Relative MFI (SRB1)
Relative MFI (E-cadherin)
ns

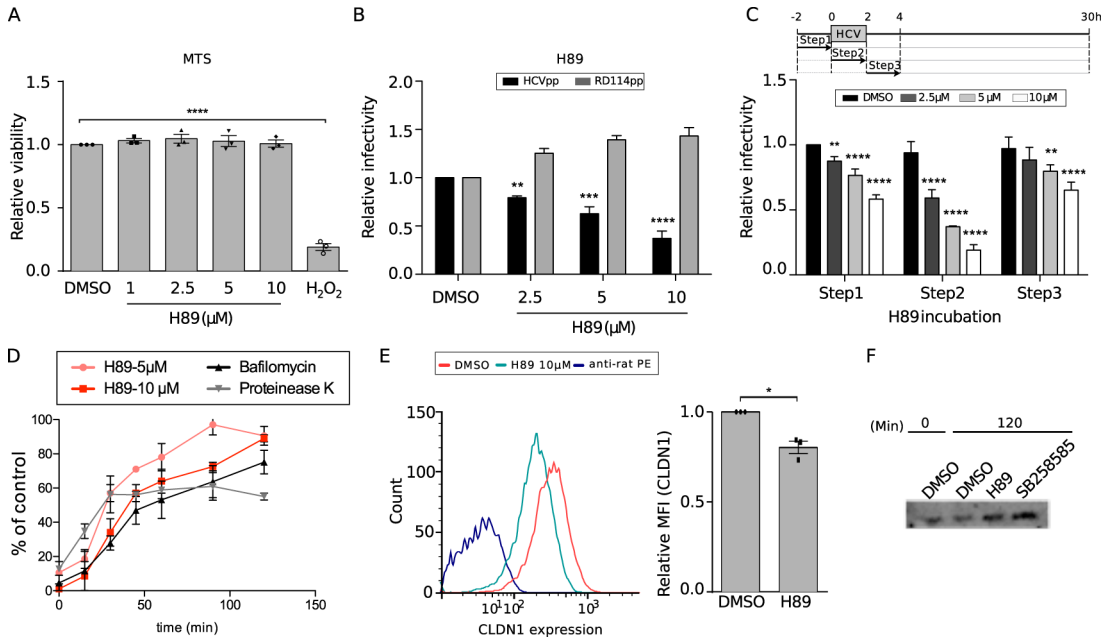
A
MTS
Relative viability
1.5
1.0
0.5
0.0
****
DMSO
1
2.5
5
10
H2O2
H89 (μM)
B
H89
HCVpp
RD114pp
Relative infectivity
2.0
1.5
1.0
0.5
0.0
**
***
****
DMSO
2.5
5
10
H89 (μM)
C
-2
0
2
4
30h
HCV
Step1
Step2
Step3
DMSO
2.5μM
5 μM
10μM
Relative infectivity
1.5
1.0
0.5
0.0
**
****
Step1
Step2
Step3
H89 incubation
D
H89-5μM
H89-10 μM
Bafilomycin
Proteinease K
% of control
100
80
60
40
20
0
0
50
100
150
time (min)
E
DMSO
H89 10μM
anti-rat PE
Count
150
100
50
0
10^1
10^2
10^3
CLDN1 expression
Relative MFI (CLDN1)
1.0
0.5
0.0
*
DMSO
H89
F
(Min)
0
120
DMSO
DMSO
H89
SB258585

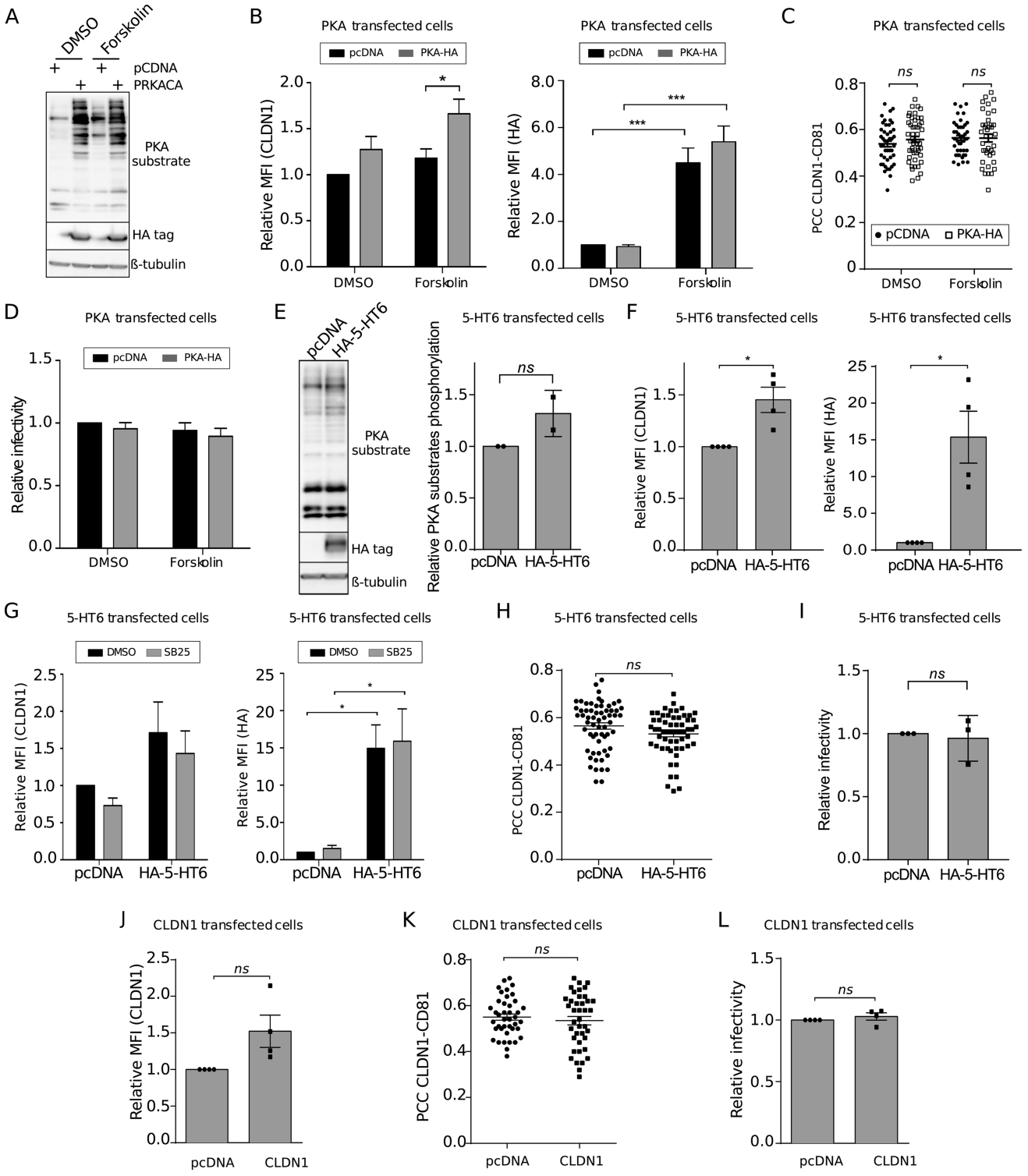
A
DMSO
Forskolin
pCDNA
PRKACA
PKA substrate
HA tag
ß-tubulin
B
PKA transfected cells
pcDNA
PKA-HA
Relative MFI (CLDN1)
DMSO
Forskolin
PKA transfected cells
Relative MFI (HA)
C
PKA transfected cells
ns
PCC CLDN1-CD81
D
PKA transfected cells
Relative infectivity
E
pcDNA
HA-5-HT6
PKA substrate
HA tag
ß-tubulin
5-HT6 transfected cells
Relative PKA substrates phosphorylation
F
5-HT6 transfected cells
Relative MFI (CLDN1)
5-HT6 transfected cells
Relative MFI (HA)
G
5-HT6 transfected cells
DMSO
SB25
Relative MFI (CLDN1)
5-HT6 transfected cells
Relative MFI (HA)
H
5-HT6 transfected cells
PCC CLDN1-CD81
I
5-HT6 transfected cells
Relative infectivity
J
CLDN1 transfected cells
Relative MFI (CLDN1)
K
CLDN1 transfected cells
PCC CLDN1-CD81
L
CLDN1 transfected cells
Relative infectivity

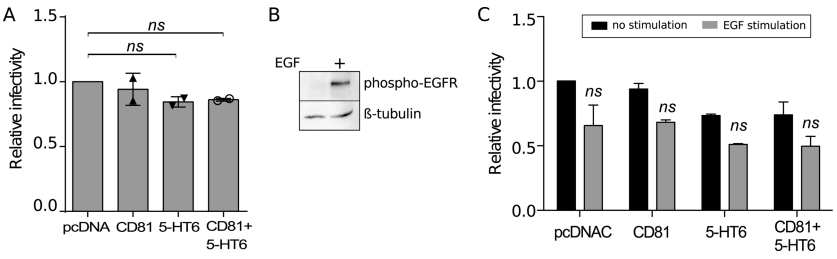
A
1.5
1.0
0.5
0.0
Relative infectivity
ns
ns
pcDNA
CD81
5-HT6
CD81+
5-HT6
B
EGF
+
phospho-EGFR
ß-tubulin
C
no stimulation
EGF stimulation
1.5
1.0
0.5
0.0
Relative infectivity
ns
ns
ns
ns
pcDNAC
CD81
5-HT6
CD81+
5-HT6

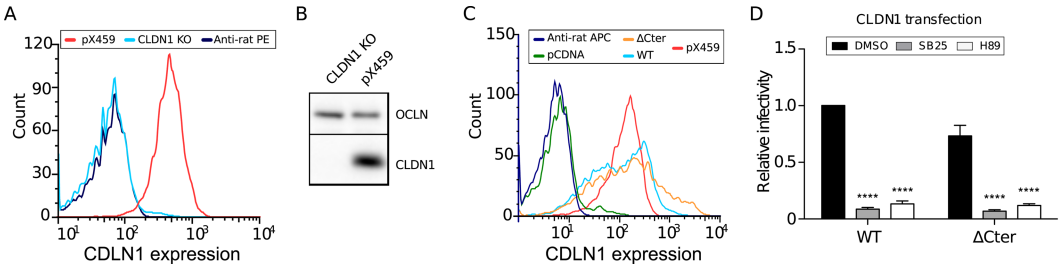
A
pX459
CLDN1 KO
Anti-rat PE
Count
CDLN1 expression
B
CLDN1 KO
pX459
OCLN
CLDN1
C
Anti-rat APC
ΔCter
pCDNA
WT
pX459
Count
CDLN1 expression
D
CLDN1 transfection
DMSO
SB25
H89
Relative infectivity
WT
ΔCter